DISCLAIMER

This report was prepared as an account of work sponsored by an agency of the United States Government. Neither the United States Government nor any agency thereof, nor any of their employees, makes any warranty, express or implied, or assumes any legal liability or responsibility for the accuracy, completeness, or usefulness of any information, apparatus, product, or process disclosed, or represents that its use would not infringe privately owned rights. Reference herein to any specific commercial product, process, or service by trade name, trademark, manufacturer, or otherwise does not necessarily constitute or imply its endorsement, recommendation, or favoring by the United States Government or any agency thereof. The views and opinions of authors expressed herein do not necessarily state or reflect those of the United States Government or any agency thereof. Reference herein to any social initiative (including but not limited to Diversity, Equity, and Inclusion (DEI); Community Benefits Plans (CBP); Justice 40; etc.) is made by the Author independent of any current requirement by the United States Government and does not constitute or imply endorsement, recommendation, or support by the United States Government or any agency thereof.

SANDIA REPORT
SAND2024-16378
Printed December 2024

Sandia National Laboratories

Strategic Petroleum Reserve Enhanced Monitoring Compendium - FY24

Dylan Moriarty

Prepared by
Sandia National Laboratories
Albuquerque, New Mexico 87185
Livermore, California 94550

Issued by Sandia National Laboratories, operated for the United States Department of Energy by National Technology & Engineering Solutions of Sandia, LLC.

Available to DOE and DOE contractors from

U.S. Department of Energy
Office of Scientific and Technical Information
P.O. Box 62
Oak Ridge, TN 37831

Telephone: (865) 576-8401
Facsimile: (865) 576-5728
E-Mail: reports@osti.gov
Online ordering: http://www.osti.gov/scitech

Available to the public from

U.S. Department of Commerce
National Technical Information Service
5301 Shawnee Road
Alexandria, VA 22312

Telephone: (800) 553-6847
Facsimile: (703) 605-6900
E-Mail: orders@ntis.gov
Online order: https://classic.ntis.gov/help/order-methods

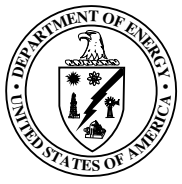

ABSTRACT

The Strategic Petroleum Reserve (SPR) is the world's largest supply of emergency crude oil. The reserve consists of four sites in Louisiana and Texas. Each site stores crude in deep, underground salt caverns. It is the mission of the SPR's Enhanced Monitoring Program to examine available sensing data to inform our understanding of each site. This report discusses the monitoring data, processes, and results for each of the four sites for fiscal year 2024.

This page intentionally left blank.

CONTENTS

LIST OF FIGURES

LIST OF TABLES

SUMMARY

This compendium is a collection of reports from throughout FY24. It discusses monitoring at all four SPR sites.

Bayou Choctaw

This year's Bayou Choctaw monitoring analysis looks at the most recent InSAR, GPS, and tiltmeter data. Results from the InSAR analysis show that subsidence rates above the SPR caverns range between -0.19 in./yr. and -0.28 in./yr. At first glance, this would seem to be greater than in previous years but the SPR's InSAR provider, TRE Altamira, realized that the previous reference location had become unstable. A new, more stable, reference monument was chosen farther from the site in Addis, Louisiana. All the InSAR results were re-analyzed with the new reference monument and subsidence trends are consistent year-over-year. Additionally, subsidence rates still exhibit seasonal variations in the southwest part of the site. This is believed to be from near surface groundwater effects. Based on the available data, there is no indication that any of the caverns have become structurally compromised.

Big Hill

Big Hill has been challenging to predict, with fluctuating subsidence rates and increasing well deformation over the past five years. This report summarizes our current understanding of the site's geology, well deformation, and surface deformation. While we explored the mechanisms behind well deformation, we found only weak correlations suggesting several possible causes. Three caverns (BH-104, BH-109, and BH-114) located on an active shear zone are experiencing significant well deformations, suggesting the shear zone's influence. However, BH-105B, which is not near any known shear zone, shows the highest well deformation at the site. The greatest subsidence rates were seen above BH-104, BH-107, BH-108, and BH-109 at just over -1 in./yr.

Bryan Mound

Bryan Mound has some of the most consistent subsidence of any of the four SPR sites - and this year is no different. The GPS and InSAR data show that subsidence is extremely linear. The tiltmeter only deviates slightly in 2021 but those movements are not seen in the previously mentioned technologies. On May 5th, 2024, BM-116A experienced a likely axial compression failure which caused a rapid depressurization. The mechanism that caused this failure is not currently reflected at the surface but we will continue to monitor the area above 116. Based on the most current surface deformation data, there is no reason to believe that any of the caverns have been structurally compromised.

West Hackberry

This year's West Hackberry monitoring analysis looks at the most recent InSAR data and reports from TRE Altamira. Data from West Hackberry shows changes in subsidence rates in 2022. There was an increase in subsidence rates in early 2022 followed by a decrease later that year. The most recent rates in 2023 show that movement has slowed to typical values seen at West Hackberry with overall subsidence

rates ranging from -0.51 in./yr. at 111 to -0.92 in./yr. above Cavern 101. A comparison between oil transfers and subsidence rates is presented and show there may be a loose correlation between the two.

NOMENCLATURE

Table 0-1. Nomenclature

Abbreviation	Definition
ALOS	Advanced Land Observing Satellite
AOI	Area of Interest
BC	Bayou Choctaw
BH	Big Hill
BM	Bryan Mound
CGG	Compagnie Générale Géophysique
CSK	COSMO-SkyMed
DOE	Department of Energy
DSM	Deep Soil Mixing
ERS	European Remote Sensing satellite
FFPO	Fluor Federal Petroleum Operations
GPS	Global Positioning System
InSAR	Interferometric Synthetic Aperture Radar
SPR	Strategic Petroleum Reserve
WH	West Hackberry

1. INTRODUCTION

Ensuring cavern integrity is paramount to a safe and operable storage facility. Although there is no direct measure of cavern integrity there are methods to infer the structural health of the cavern field. These methods include monitoring quantities like surface deformation, cavern shapes, and cavern pressures. This report considers each available dataset, presents an analysis, and discusses our best understanding of cavern integrity at all SPR sites. Information within this report will look at the most recent data. For more historical information please see previous Strategic Petroleum Reserve enhanced monitoring compendia [1, 2].

For the Strategic Petroleum Reserve (SPR) to accomplish its mission we need to ensure the caverns holding the oil are structurally stable. One way to monitor this is observing the change in elevation at the surface deformation above the caverns. Most of the SPR sites - and the gulf coast at large - exhibit a loss of elevation over time. This phenomenon is typically referred to as subsidence. From subsidence, we can infer the structural integrity of the cavern field below. This is because stresses and movements in a cavern are eventually translated to the surface as subsidence. Subsidence is normal and expected, however, if the rates change unexpectedly or are too high it can be cause for concern. This is why the SPR program has been monitoring subsidence for over four decades and have recently added state-of-the-art monitoring techniques.

Traditionally, surface deformation had been measured by annual or biennial elevation surveys using level-and-rod. In FY20, the SPR decided to monitor ground movement using InSAR, a satellite-based technique. This method collects thousands of times more data and provides greater insight into the dynamics of surface deformation. Figure 1-1 shows the surface deformation through time for all four SPR sites for comparison. The figure shows the most recent InSAR data for each site except Bryan Mound - the most recent InSAR analysis used a smaller time window to better observe recent events at the site. The colored area represents the bounds of the 10th and 90th percentiles, while the bold line within shows the median value.

In addition to surface deformation, there could be special considerations at each site that may require other data streams. For example, at Big Hill we examined geological and well data alongside surface deformation in an attempt to better understand the mechanisms of well deformation.

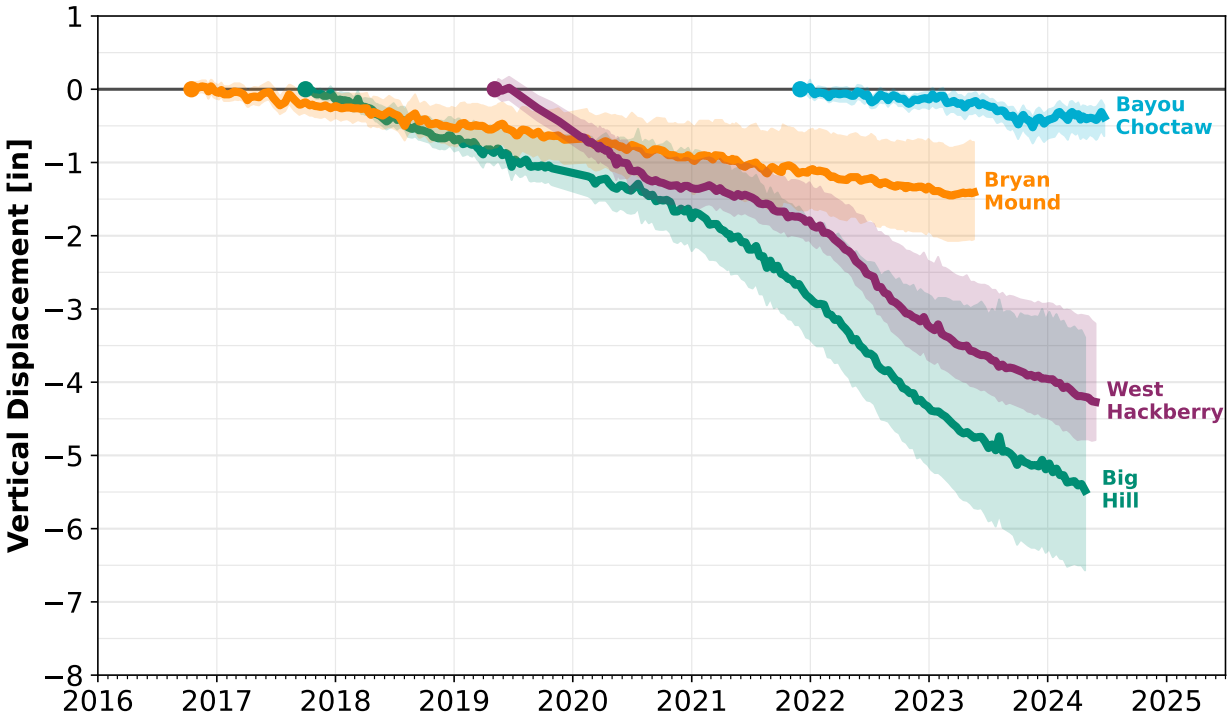

Figure 1-1. Comparison of surface deformation over time at all four SPR sites with Big Hill being highlighted. The colored area represents the bounds of the 10th and 90th percentiles, while the bold line within shows the median value. All measurements were taken with InSAR and have different start and end dates.

2. BAYOU CHOCTAW

2.1. Introduction

Bayou Choctaw has long been the site with the least amount of subsidence, but is also home to BC-004 - a cavern that protrudes into the caprock near the center of the site. This analysis considers each available dataset, presents an analysis, and discusses our best understanding of cavern integrity at Bayou Choctaw. Information within this report will look at the most recent surface deformation datasets.

2.2. Monitoring Technologies

There are three surface monitoring technologies used at Bayou Choctaw: InSAR, GPS, and tiltmeters. Each technology has it's own sampling area, frequency, and quantity measured but, ultimately, each instrument is used to observe surface deformation. Surface deformation is used to infer stress changes within the caverns. If stresses change in a cavern, those stresses propagate to the surface and typically result in surface deformation. This deformation is usually in the downward direction and referred to as subsidence.

InSAR stands for Interferometric Synthetic Aperture Radar and is the primary method for monitoring surface deformation at the site. It is a satellite based technology that can measure sub-millimetric changes in surface elevation. The SPR has been using InSAR at Bayou Choctaw since January 2019. Prior to InSAR, the site was measured using digital level-and-rod surveys. In the summer of 2022, the SPR adopted 2D InSAR at Bayou Choctaw. In total, the SPR has 177 surveys, or images, of Bayou Choctaw since InSAR was deployed. Since InSAR satellites have near polar orbits, they pass over the site using two trajectories, ascending and descending. When the satellite is passing over the site in a north to south trajectory, it is called a descending orbit. Conversely, when the satellite is imaging the site in a south to north trajectory it is referred to as ascending. Ascending and descending orbits pass over the site at different angles and will observe movement directly towards or away from the satellite. This is referred to as 1D InSAR. Information from both orbits can be combined to produce 2D InSAR. This type of InSAR calculates true vertical movements and horizontal ground movements in the east-west direction.

Realtime sensing instruments are also located over key caverns. GPS measures elevation change while tiltmeters observe change in tilt over a specific location. They are typically used in conjunction with one another and serve as redundancies for the other. These instruments are constantly monitoring but record measurements hourly.

2.3. Surface Deformation

2.3.1. InSAR

The primary method for measuring surface deformation at the site is satellite-based InSAR. InSAR data at Bayou Choctaw were processed by TRE Altamira. The results used in this report are taken from two TRE Altamira reports. Both reports are titled "Analysis of Ground Displacements over the Bayou Choctaw Salt Dome" but one was submitted to the SPR in November 2023[3] and the other in February 2024[4].

2.3.1.1. Reference Monument Change

The biggest change seen in the past two reports was a change to the reference monument. During the previous InSAR analyses, TRE Altamira discovered that the initial reference point had become unstable. This led to a search for a secondary location suitable for the Bayou Choctaw site. They found a location within Addis, Louisiana - approximately 3.7 miles NE of the site. The change in reference point farther from the dome also allowed for a larger area of interest (AOI). The reference monument and the change in AOI can be seen in Figure 2-1. In the figure, the current reference monument is represented as a red dot at the top of the figure. The AOI used prior to the September 2023 analysis is marked by a green rectangle while the new AOI is shown as a pink rectangle. All InSAR data presented within this report use the new reference location and AOI. A comparison of subsidence rates before and after the reference location change can be found in Appendix A.1.

2.3.1.2. 1D InSAR

Initially, the SPR opted to observe Bayou Choctaw using 1D InSAR measurements. The first available image was taken on January 9, 2019 and the most recent report has 107 analyzed ascending images. The 1D imagery from the ascending orbit is shown in Figure 2-2. The boundary of the Bayou Choctaw salt dome at a depth of 5000 ft. is shown as a gray line. The boundary of the SPR site is a yellow dotted line and the SPR caverns are labeled with black outlines. InSAR shows that there is little overall movement between January 9, 2019 and December 21, 2023. There is some subsidence occurring outside the SPR boundary. This particular subsidence is from surface construction on an adjacent cavern operator's site.

In the summer of 2022 the SPR adopted 2D InSAR. 2D InSAR is created using data from two satellite orbits, ascending and descending. Although the decision to implement 2D InSAR didn't occur until 2022, there were images of the site available back to December 2021. Data from the 1D descending orbit can be seen in Figure 2-3. Most of the parameters between the two orbits are the same other than the angle the image was taken and the timeframe of the available images. There have been 70 descending images taken since the first in December 2021.

The biggest difference between the two 1D datasets are the visibility of "hotspots" or areas of higher subsidence. These locations that show higher subsidence rates correspond to recent construction in and around the SPR site where soil compaction is the main driver of surface deformation. The area of higher subsidence between Cavern 004 and Cavern 101 is a newly constructed lay-down yard while the higher subsiding area above Cavern 20 is the location of a trailer installed for the LE2 project. There has also been

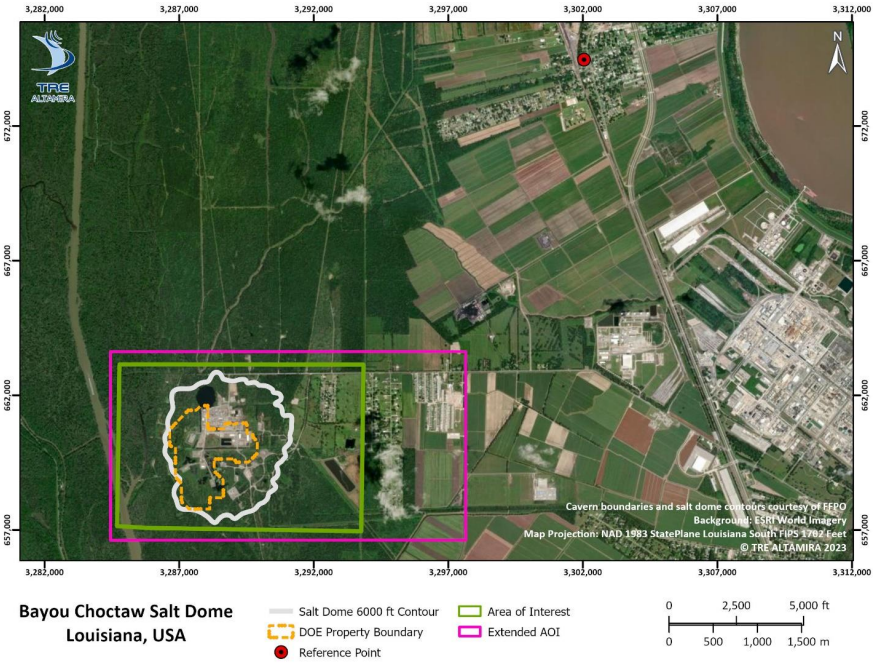

Figure 2-1. Comparison between the areas of interest at the Bayou Choctaw SPR site. The reference monument is shown with the red dot within Addis, Louisiana. The green rectangle shows the previous area of interest while the pink shows the current area of interest. From TRE Altamira Report.

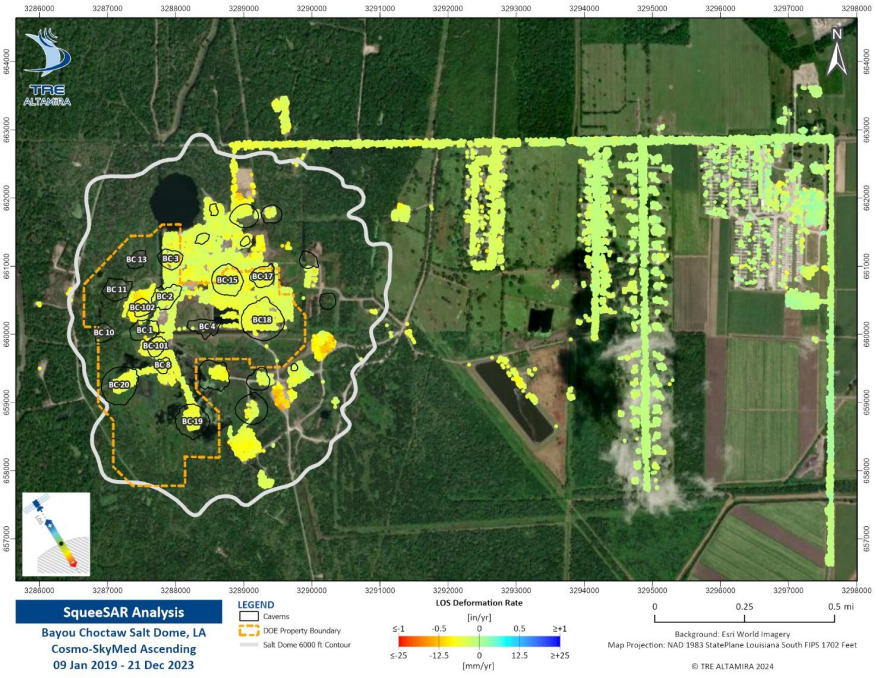

Figure 2-2. 1D ascending InSAR at Bayou Choctaw between January 2019 and December 2023. From TRE Altamira Report.

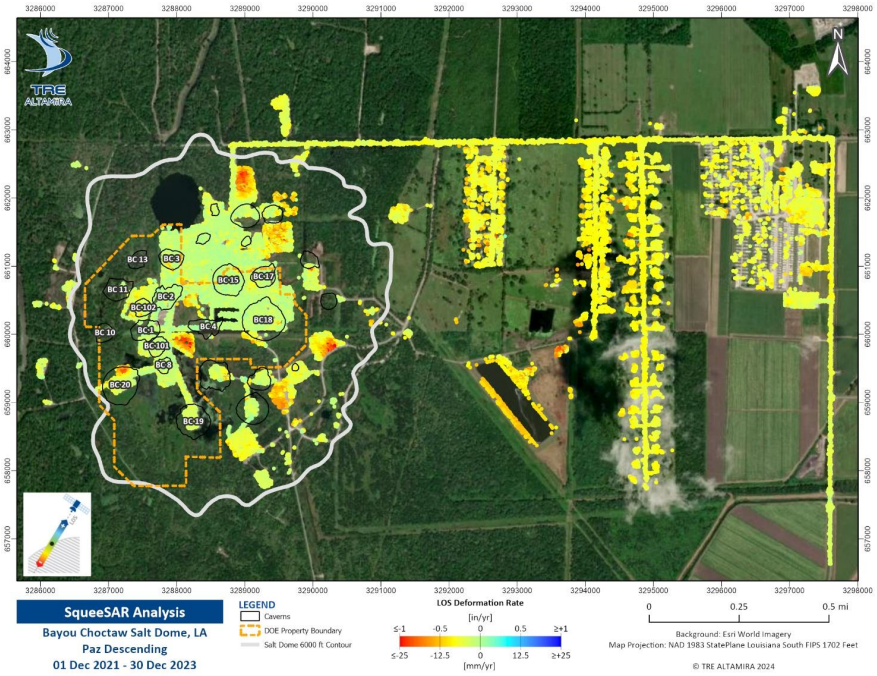

Figure 2-3. 1D descending InSAR at Bayou Choctaw between December 2021 and December 2023. From TRE Altamira Report.

some offsite construction that corresponds to higher subsiding areas outside SPR property. As the soil becomes more compacted in these areas, we expect to see less subsidence in these areas.

It should be mentioned that these "hotspots" are not seen in the ascending data. This is likely due to the time frame for imagery. The ascending data began before construction at some of these sites. Once construction occurred, it likely made those points too unstable for the satellite to track and, therefore, there is no data in these locations.

2.3.1.3. 2D InSAR

Ascending and descending orbits from the same satellite can be used simultaneously to calculate 2D InSAR results. In this case, two similar satellites - Cosmo-SkyMed & Paz - were used to calculate the results from ascending and descending orbits. Since data from both orbits need to be used, 2D results are only available in locations where both satellites have reflections. In this case, the coverage is more similar to the ascending results. Overall vertical displacement data from the 2D results are presented in Figure 2-4. 2D data are only available between December 2021 and December 2023.

Like the ascending and descending data, there is only slight overall subsidence seen at the site. In addition, the rate of subsidence is largely consistent across the site. This is in contrast to the other SPR sites that show differential subsidence rates. Areas of higher subsidence are only seen off the Bayou Choctaw SPR site.

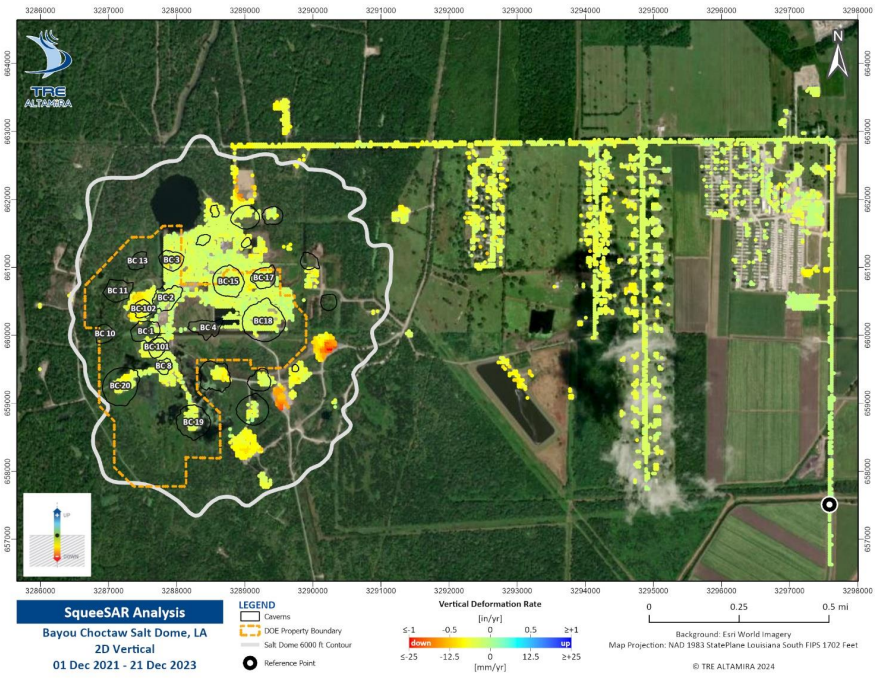

Figure 2-4. 2D vertical InSAR at Bayou Choctaw between December 2021 and December 2023. From TRE Altamira Report.

Figure 2-5 shows the calculated horizontal movement in the east-west directions. Most of the AOI does not show any horizontal movement in the E-W direction; however, areas near the center of the Bayou Choctaw dome show slight easterly movement. Although the movement is small, we will continue to monitor these trends. It is important to remember that we can only see movement in the east-west plane direction and have no indication of north-south movement or total horizontal movement. Without the north-south component of horizontal movement it is difficult to infer the mechanisms that are causing the horizontal movement.

Other SPR sites with 2D InSAR seem to exhibit east-west horizontal movement towards the center of the cavern field (Big Hill) or towards the area of highest subsidence (Bryan Mound). Bayou Choctaw does not show a clear trend in the east-west plane of movement.

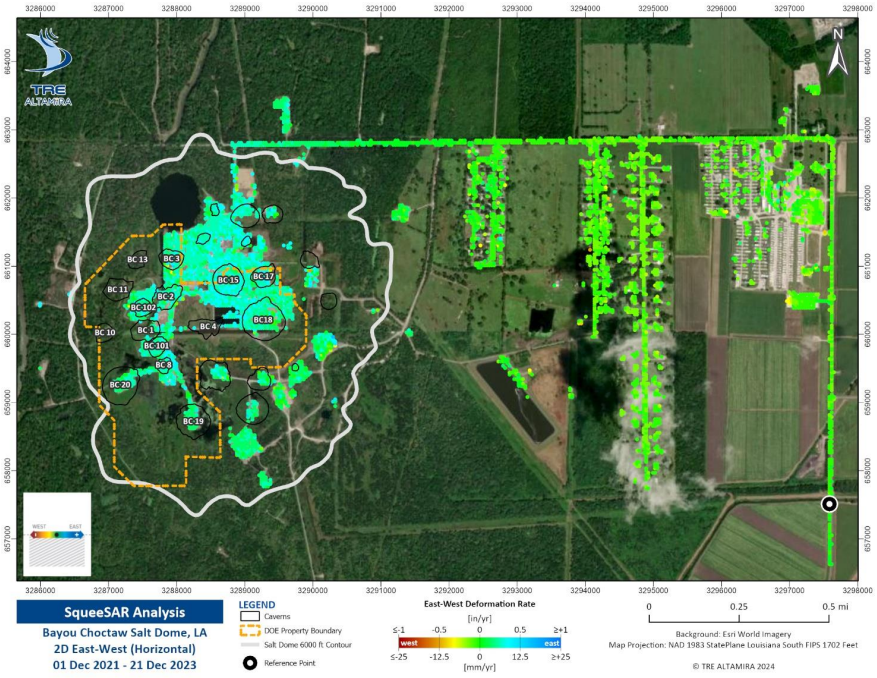

Figure 2-5. 2D horizontal InSAR at Bayou Choctaw between December 2021 and December 2023. From TRE Altamira Report.

2.3.2. Realtime Sensing

In addition to InSAR monitoring at the site there are also four instruments measuring in realtime - two GPS instruments and two tiltmeters. The instruments are placed strategically above Caverns 004 and 020. Cavern 004 is a cavern in the center of the site that protrudes into the caprock (no salt cap). Cavern 020 is a deeper cavern but nears the edge of salt. Both caverns are monitored closely due to their proximity to the edge of the salt dome.

2.3.2.1. Cavern 004

Cavern 004 has a tiltmeter and GPS. Both instruments were installed in 2013, however, historical tiltmeter measurements before May 2016 were unavailable at the time of writing. The results for the GPS are shown in Figure 2-6. The hourly measurements are shown as transparent black dots. A median filter with a window of a month was applied to the data. The filtered data is represented by a red line in Figure 2-6 and clearly shows a seasonal trend with a higher elevation in the winter and lower elevations in the summer. Although this seasonal variation occurs each year, the overall relative movement of the GPS is effectively zero.

Figure 2-7 shows the tiltmeter measurements above Cavern 004. Like the GPS above Cavern 004, there are seasonal variations will little overall movement. Northing and easting measurements are shown in orange and blue, respectively. Both the corrected measurements and the filtered measurements are shown in the figure. It should be noted that the data presented in Figure 2-7 were corrected to account for

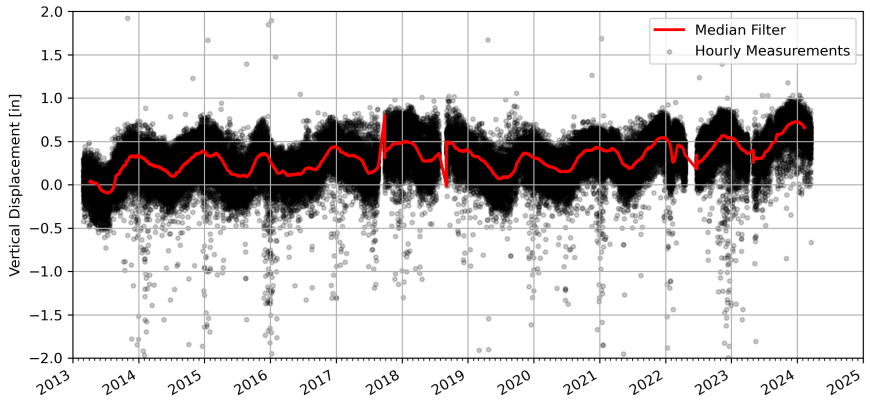

Figure 2-6. Hourly GPS measurements above Bayou Choctaw Cavern 004. The original measurements are shown as transparent black dots while the filtered elevations are shown with a red line.

tiltmeter disturbances. The original measurements and the corrections applied to the data are presented in Appendix A.2. Corrections were based on expert opinion.

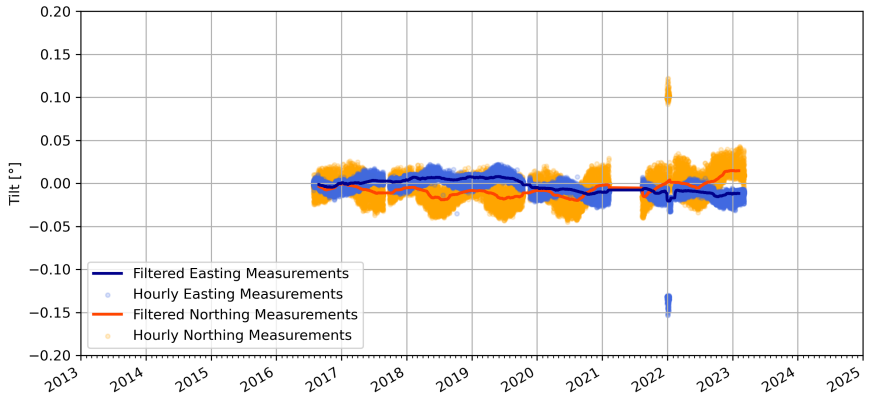

Figure 2-7. Hourly tiltmeter measurements above Bayou Choctaw Cavern 004. The corrected northing measurements are shown in orange while the adjusted easting measurements are shown in blue.

There are several data artifacts that show at the end of 2021 and the beginning of 2022. At the end of 2021, there was a jump in data that needed to be corrected. This would indicate the tiltmeter was disturbed during this time. The resulting artifacts could have been from reinstallation or subsequent adjustment of the tiltmeter or its base. The other datatypes suggest these readings were not due to surface deformation but, rather, temporary disruption to the tiltmeter or its base.

During this year's analysis, we also discovered that the tiltmeter at Cavern 004 had stopped recording data in early 2023. The SPR is currently working with the data host, Sensemetrics, to figure out the cause of the failure.

2.3.2.2. Cavern 020

In 2017, a GPS and tiltmeter were installed above Cavern 020. GPS measurements, presented in Figure 2-8, show a similar pattern to the GPS above Cavern 004 - higher in the winter and lower in the summer little change year-over-year. Like the Cavern 004 tiltmeter, it looks as though the Cavern 020 GPS stopped recording data in early 2023. Investigations are ongoing to see why the data are not being recorded.

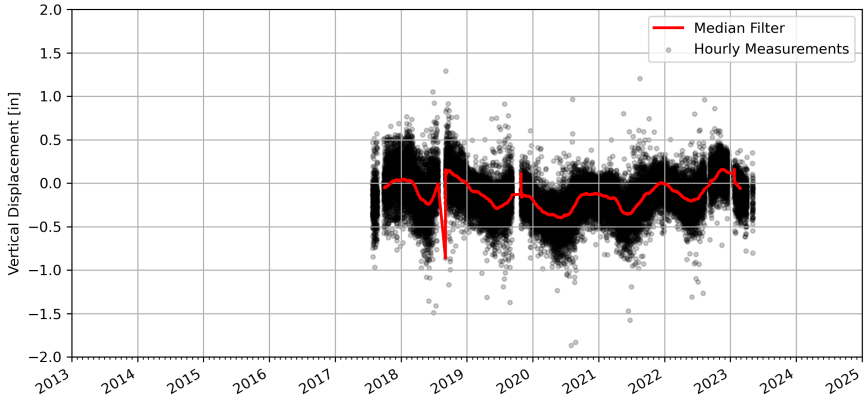

Figure 2-8. Hourly GPS measurements above Bayou Choctaw Cavern 020. The original measurements are shown as transparent black dots while the filtered elevations are shown with a red line.

The tiltmeter measurements for Cavern 020 are shown in Figure 2-9. The methodology for correcting the measurements are similar to those used for the Cavern 004 tiltmeter described in Section 2.3.2.1. The tiltmeter trends are similar to the ones seen in the Cavern 004 tiltmeter - small seasonal movement with no overall displacement - but the tiltmeter begins to fail in 2020. The erroneous measurements after 2020 are not believed to reflect actual movement. There is no other information that corroborates this movement and this particular make of tiltmeter has exhibited several failures at other SPR sites.

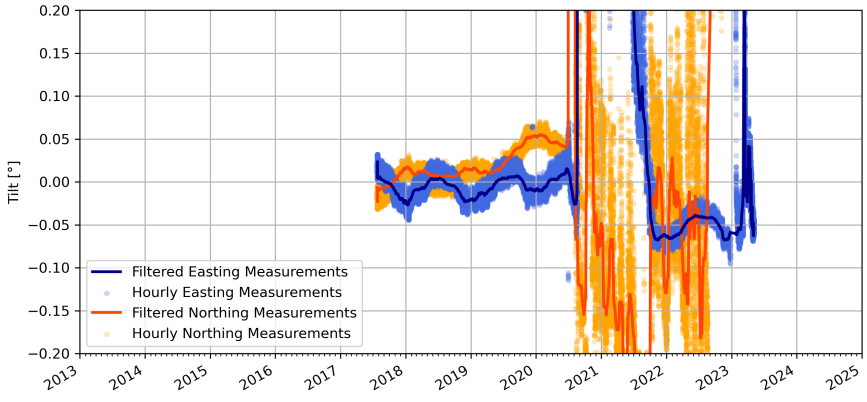

Figure 2-9. Hourly tiltmeter measurements above Bayou Choctaw Cavern 020. The corrected northing measurements are shown in orange while the adjusted easting measurements are shown in blue.

2.4. Comprehensive Monitoring

2.4.1. Correlation to Oil Transfers

Although there have been oil transfers at the Bayou Choctaw, there has been no discernible deformation at the surface that coincides with site activity. Subsidence at Bayou Choctaw has always been near zero with little differential subsidence. As such we have not seen any correlation between oil transfers and subsidence.

2.4.2. Seasonal Movements

Results from InSAR, GPS, and tiltmeters show small seasonal movement at Bayou Choctaw. The most updated seasonal movements are shown in Figure 2-10. The figure shows the amplitude of the seasonal variations at the site. Pink areas show the areas with the highest seasonal amplitude while areas in yellow show little to no seasonal variations.

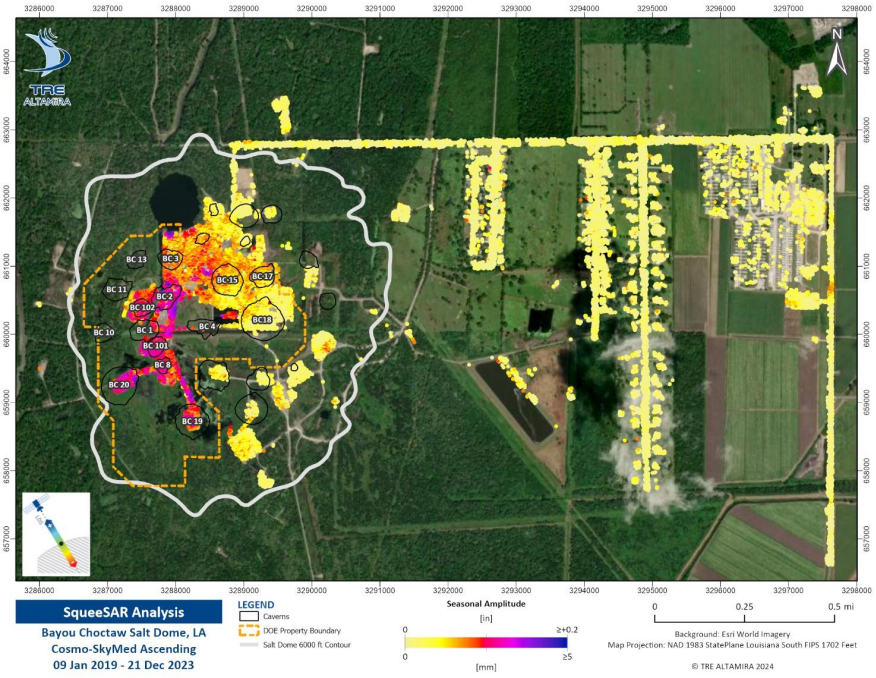

Figure 2-10. Seasonal amplitude at Bayou Choctaw calculated from ascending InSAR data. From TRE Altamira Report

Figure 2-10 shows the areas with the highest seasonal variation are located in the southwest portion of the site. This area is a swampy area with less engineered soils beneath infrastructure indicating variations are due to near-surface groundwater effects. This topic is further investigated in the report by Valdez and Moriarty[5] which concludes:

> *"The most apparent correlation between the seasonal pattern at Bayou Choctaw is the shrink-swell cycle behavior between the soil and water near the surface. The soil around Bayou Choctaw*

has expansive soil properties, such as high clay content, high water content availability, higher organics percentage, and poor drainage in areas without engineered soil. These properties govern how water moves and is stored in the soil near the surface."

Our best assessment concludes that most of the movement is occurring near surface. Data from this year's InSAR, GPS, and tiltmeter instruments continue to support the findings in that report.

2.5. Bayou Choctaw Conclusions

This year's InSAR data changed slightly with the change in reference monument. Instead of the slight upward movement seen in previous year's data, we now see slight overall subsidence at the site. Despite the change in overall subsidence we still see the seasonal movements which have not changed in amplitude. Additional information from GPS and tiltmeters above Caverns 004 and 020 also show the main driver of surface movement at Bayou Choctaw is believed to be from near-surface, groundwater effects. It should be noted that data from the Cavern 004 tiltmeter and the Cavern 020 GPS have stopped being reported in the Sensemetrics application and investigations as to the cause are ongoing. Given the data, there is no reason to believe that any of the caverns at Bayou Choctaw have lost structural integrity.

3. BIG HILL

3.1. Introduction

In the past decade, Big Hill has experienced significant well deformation in several wells in the western half of the site. This deformation has led to the decommissioning of BH-105B and there is concern that well deformation will continue in the other wells until they, too, become unusable. In this report, we are reviewing the most recent geology, multi-arm caliper, and subsidence data to see if we can find correlations that could indicate a driving mechanism for well deformation at Big Hill. Additionally, the rate of deformation will be considered to determine which wells are likely to have a longer serviceable lifetime.

3.2. Big Hill Geology

Understanding the Big Hill spine history may lend towards a better understanding of well deformation patterns. Salt domes are thought to move upwards in multiple discrete cumulations, called spines, at different rates over various timelines and not as one massive unit. Spines are separated by boundary shear zones that consist of anomalous regions that vary in composition and physical properties from the main salt body [6]. Internal structure, such as boundary shear zones, are likely to have influence on cavern shape, integrity, operations, and perhaps well integrity. Individual spine bodies can also shift in directions and be forced geologically to move in azimuths other than vertical, which could initiate shearing ultimately impacting well stability. Big Hill spine interpretations were initially conducted in 1988 and updated in 2005. Considering the ongoing Big Hill well behavior and lack of causal understanding we have revisited these past interpretations to ultimately assess if any relation between multiple site and operation datasets may correlate to geologic influences. The historical spine interpretations are summarized below.

In 1988, with the drilling of the 28 Big Hill cavern wells, a NE-SW shear zone across the cavern field was identified during the updated geologic characterization study [7]. A shear zone is a boundary between spine complexes. This major shear zone was mapped using neutron density logs acquired in each of the 28 cavern wells. Anhydrite layers were identified and correlated between the cavern wells. The boundary shear zone (Figure 3-1) is located between caverns 103 and 104, 108 and 109, and 113 and 114.

The 2005 recharacterization[8] of the dome identified up to 12 spines. Methodology consisted of inclusion of all new and historical sulphur, oil, and gas wells within an expanded study area. Both caprock and salt tops were remapped, and shear zones were identified by structural contour reentrants; the caprock records the accumulation of insoluble anhydrite from the salt mass as the salt rises and is dissolved when it intercepts the groundwater. Figures 2 and 3 display the inferred spines. The major boundary shear zone identified in 1988, cutting across the cavern field, was also identified in the 2005 mapping and extends across the entire dome trending NE-SW (Figure 3-4).

In addition to the remapping of the caprock and salt, Rautman and others (2005) also created a series of isopach maps of the sedimentary layers surrounding and abutting the dome. Isopach maps were used to interpret whether sedimentation occurred before or during salt intrusion and if during intrusion which region of the salt dome was more active historically through time. This exercise also informed that the NE-SW boundary shear zone, recognized in both studies, appears to have been active throughout much of the Big Hill dome history.

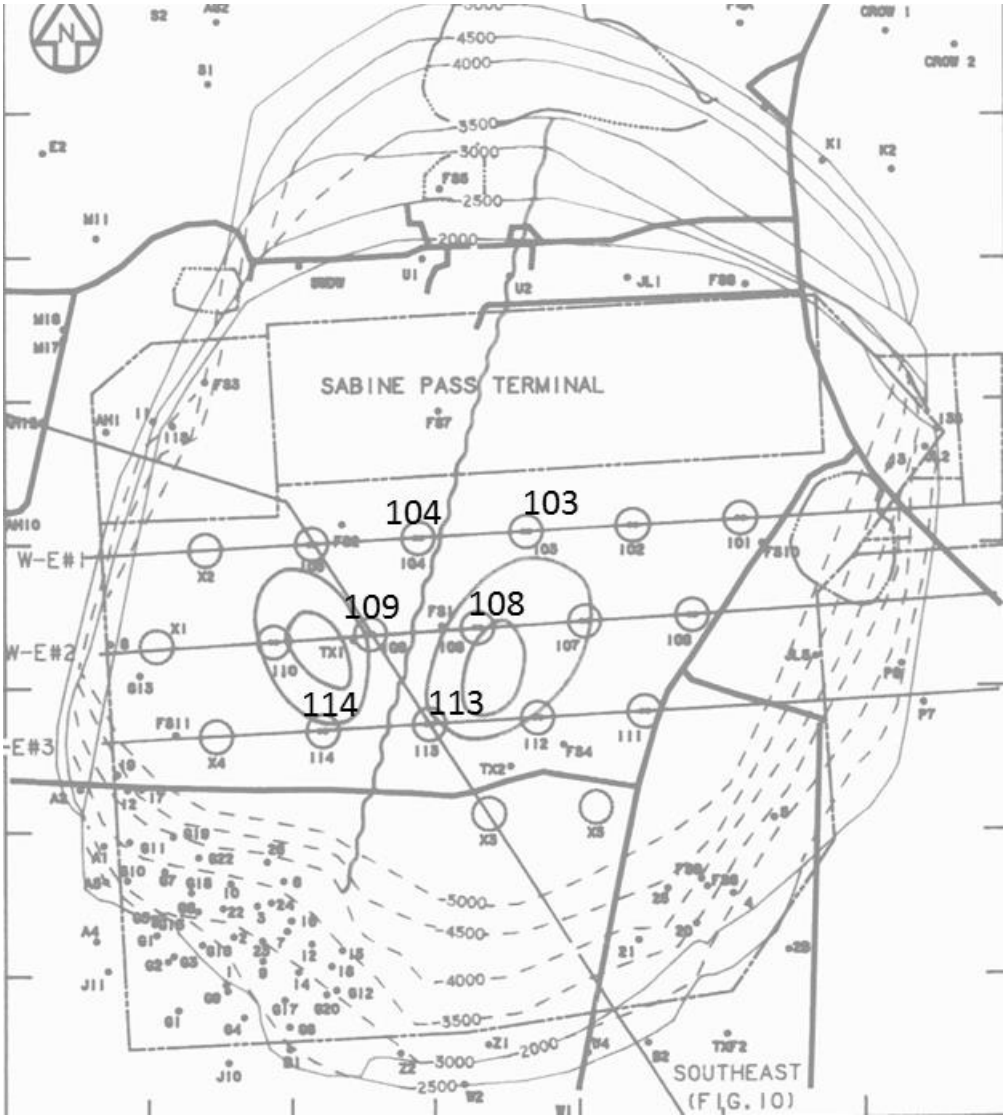

Figure 3-1. 1988 Big Hill Top-of salt structure contour map with cavern locations. Location of mapped boundary shear zone is indicated by wavy line. From Magorian and Neal, 1988, Figure 1.

3.2.1. 2005 Study Interpretation

The overlying caprock is thought to represent a record of the underlying salt movement history. The caprock consists of insoluble impurities, typically anhydrite, left behind after dissolution of the rising salt

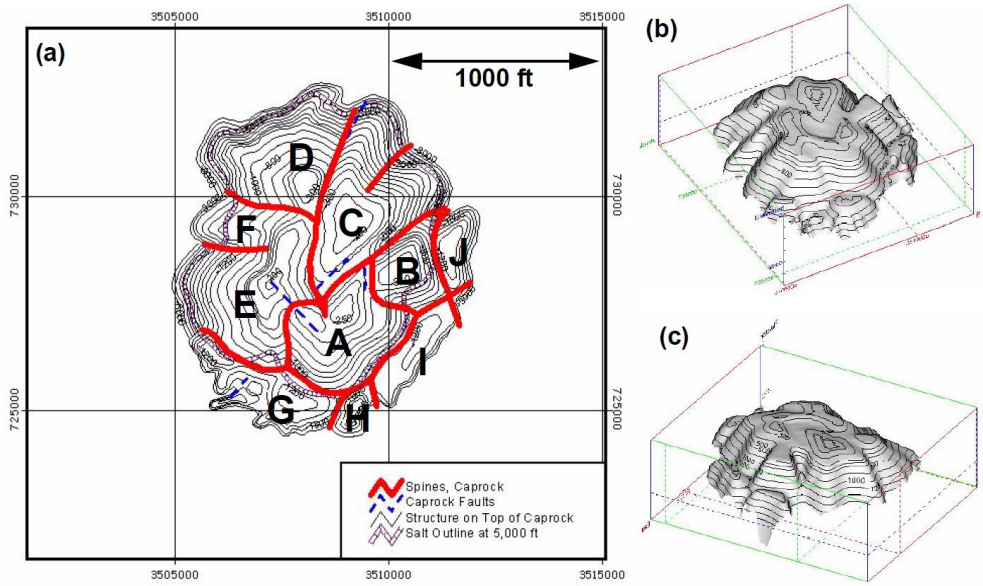

Figure 3-2. 2005 caprock structure-contour map showing subdivision of spines in red. Computer-generated perspective views to the right. From Rautman et al. 2005, Figure 4.

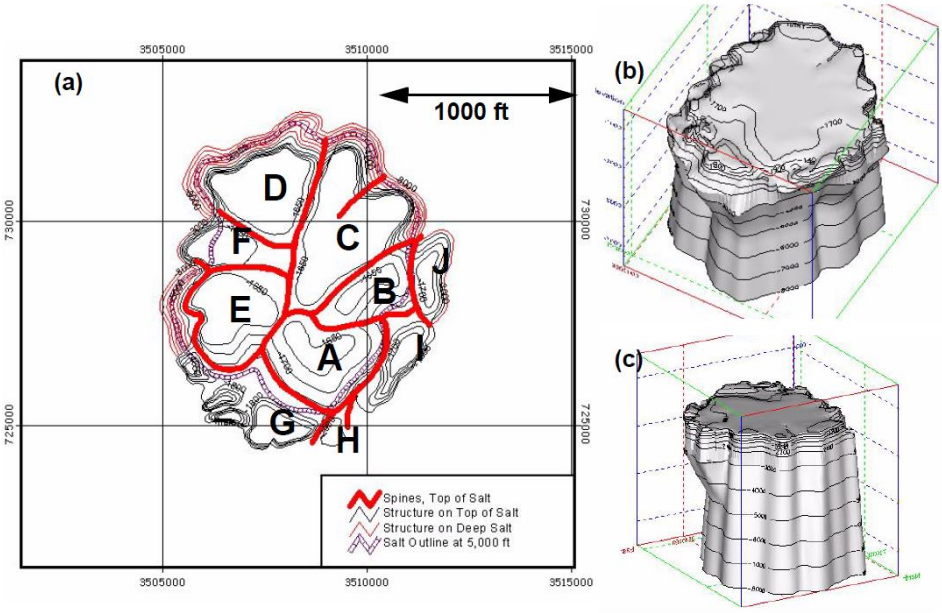

Figure 3-3. 2005 salt structure-contour map showing subdivision of spines in red. Computer-generated perspective views to the right. From Rautman et al. 2005, Figure 5.

by encountered groundwater. The pattern of the mapped caprock thickness indicates what regions of the underlying salt dome were more active than others.

The Big Hill caprock structure-contour map (Figure 3-2) indicates significant thickness at the center of

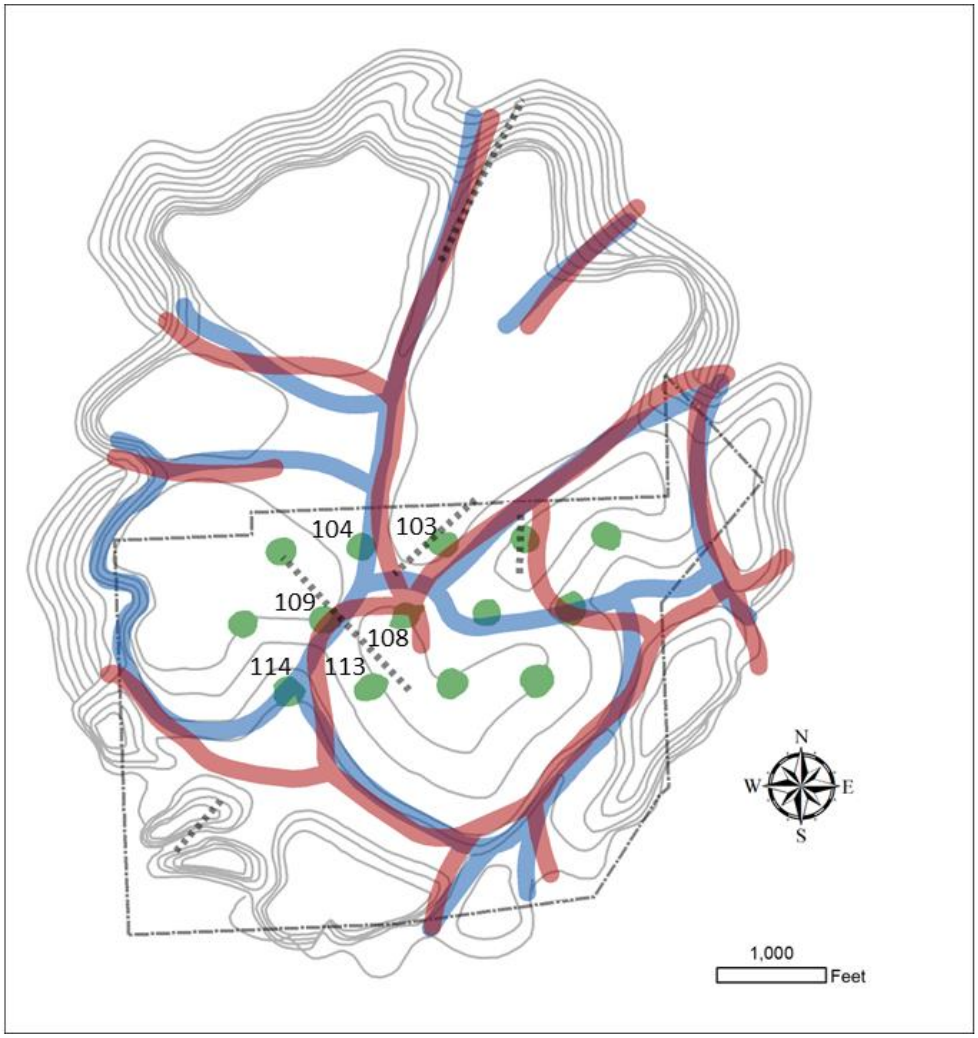

Figure 3-4. 2005 salt structure-contour map with cavern locations in green with interpreted subdivision of spines from both the salt (blue) and caprock (red) maps. Note prominent boundary shear zone mapped through the cavern field near caverns 103-104, 108-109, and 113-114 also coincides with the major shear zone mapped in 1988 (Figure 3-1).

the dome implying this region has seen the greatest cumulative upward salt movement over time. The thick center is surrounded by a ring of thinner caprock suggesting shorter time of salt activity.

The salt structure-contour map (Figure 3-3) exhibits very little topographic expression, which is expected as salt is continually being dissolved. Any expression of relief suggests a region of active salt activity and represents current conditions. Interpretation of the Big Hill salt suggests a currently static dome interior surrounded by relatively active regions on the periphery (Figure 3-3 (b)).

The outer thinner ring of caprock overlaps the major salt overhang along the southern and eastern margins of the dome (Figure 3-5). The mapped salt overhang exhibits subtle structural relief. The theory is the continued rise of salt toward the north could no longer be accommodated by vertical movement due to large resistant mass of caprock. The thick caprock forced the rising salt outward along the eastern and southern margins. [8]

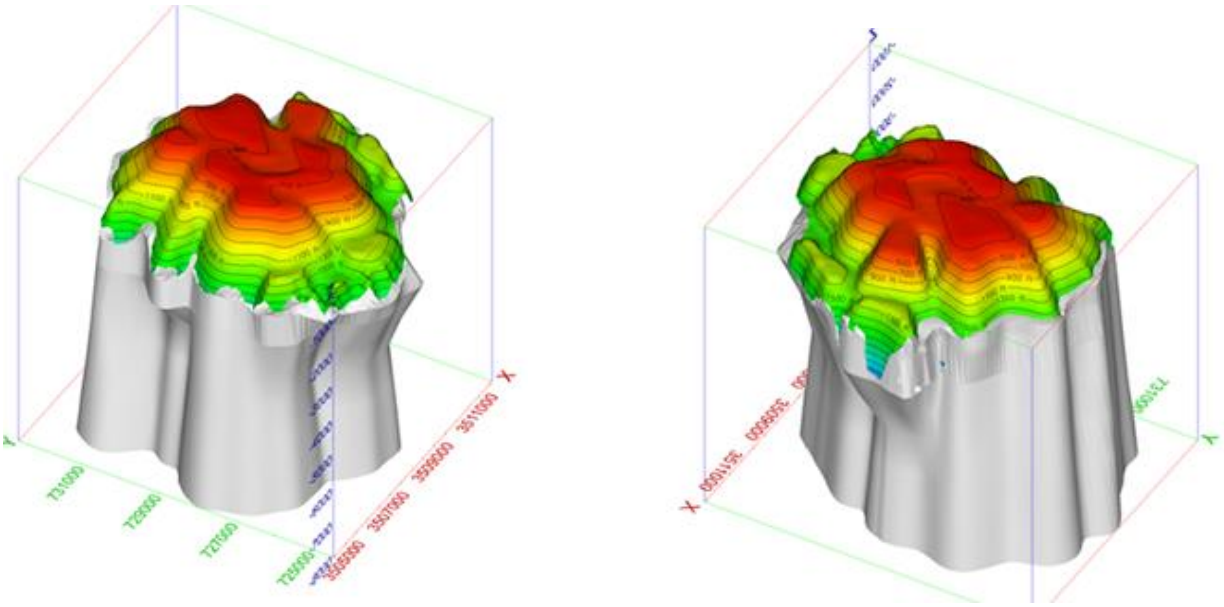

(a) View from SW (b) View from NE

Figure 3-5. Three-dimensional perspective views of the combined caprock and salt surfaces. (Similar representation as Figure 6 in Rautman et al., 2005.

On the western side of the dome there is a small overhang, at a shallower depth than the other surrounding overhangs mapped to the south and east, with no correlating overlying independent caprock cumulation (see Figure 3-5a, SW view). Both the shallow depth and lack of corresponding isolated caprock record suggest this region may be the youngest and represents a short period of activity. (From Rautman and others, 2005 DRAFT SAND; never published)

3.2.2. NE-SW Boundary Shear Zone

To summarize, at least 12 spines are identified that represent the current dome configuration. There is one major boundary shear zone that cuts across the entire dome and cavern field from the northeast to the southwest supported by density well logs, top-of-caprock/salt mapping, and historical inference from mapped isopach maps of the surrounding sedimentary layers. This major boundary shear zone cuts through the Big Hill cavern field between caverns 102-104, 108-109, and 113-114.

Other records support the presence of the NE-SW trending boundary shear zone. A 1993 caprock top-of structure contour map [6]; Figure 3-6) illustrates a graben fault (i.e., apparent sunken fault block) located essentially above the location of the underlying NE-SW boundary shear zone. The two parallel faults making up the graben complex, within the caprock, meet at the underlying salt surface at the location of the mapped boundary shear zone. The caprock faults mapped were "seen" from 2D seismic lines shot in 1992. The graben fault is interpreted as active, which suggests the underlying salt is still rising.

Cavern development historical records [6] noted events that occurred during cavern creation that support the presence of the boundary shear zone. Boundary shear zones or "anomalous feature" are defined [9] by a deviation from generally pure salt and may exhibit inclusion of other rock materials, change in crystal

size and permeability, brine or hydrocarbon pockets, and gas outbursts. These zones may be a few feet to several hundred feet wide and extend linearly from between a few hundred feet to the entire length of the dome. During the leaching of **Cavern 114, 150 barrels of hydrocarbons were encountered**. The hydrocarbons were thought to come from an isolated pocket within the salt. Cavern 114 is near the edge of the dome, adjacent to the south overhang where oil production had occurred. The hydrocarbons were most likely encapsulated within the salt during upward movement of salt along the shear zone. During sump development **Cavern 103 experienced excessive corrosion caused by highly alkaline brine**. High alkalinity brines have been associated with anomalous zones [6]. During leaching of **Cavern 109 high pressure buildup occurred due to higher-than-normal gas production**, which could result from the cavern's close proximity to the shear zone. No other major occurrences were noted during leaching of the other 11 caverns.

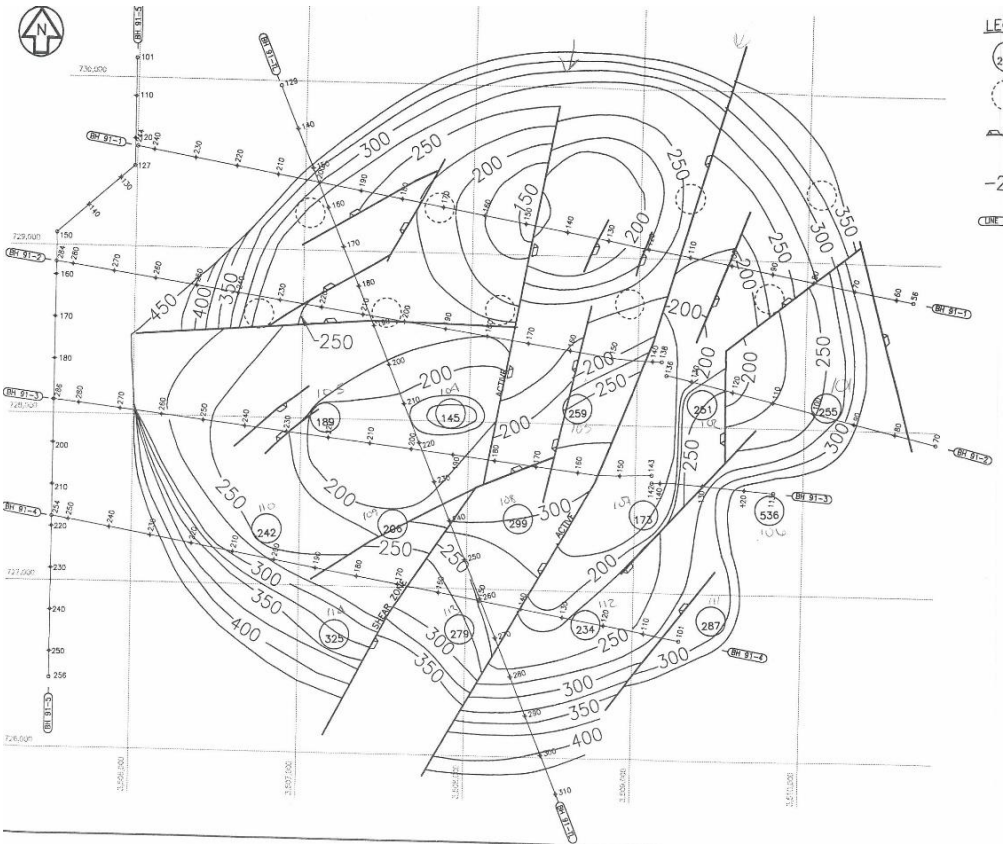

Figure 3-6. Big Hill top-of caprock structure contour map interpreted from 2D seismic, from Neal et. al, 1993, Figure 5.

3.2.3. Recent Salt Activity Summary

Geologic interpretation infers that recent activity of the Big Hill salt dome consists of up to 12 individual spines. The overlying caprock is approximately 1200 feet thick near the central part of the dome. It is thought that due to the massive caprock the salt can no longer move vertically and is being thrust out horizontally forming overhangs to the south and east of the salt dome. The graben fault present across the

caprock is interpreted to be active, which also suggests the underlying salt shear zone is active too causing the faulting above.

3.3. Multiarm Caliper Review

This section presents a condensed review of conclusions drawn from analysis of Multi-arm Caliper (MAC) well logging data. MAC data provide a measurement of the interior geometry of the innermost cemented casing of the well. This is provided via radial measurements made using a series of feeler arms (Figure 3-7) of the downhole logging tool as it is raised up through the well. This information can then be used to assess the location and magnitude of radial distortion of the casing. Several wells at the Big Hill site have experienced severe casing deformation and the MAC logs of these wells are paramount in understanding the magnitude and rates of the deformation.

In general, logging a well using a MAC tool is relatively uncomplicated. The tool is raised through the casing and the radial displacement of the feeler arms is measured as a function of depth. Recently, the MACs run at the Big Hill site have included a gyroscopic instrument in the tool string. This allows the MAC data to be oriented with respect to true cardinal directions which is useful in interpretation of the data.

Since the logging vendor for SPR MACs changes periodically, which leads to differing interpretations of the MAC data through time, the Sandia National Laboratories (SNL) SPR group has developed its own MAC data analysis procedure. This provides a consistent set of analysis variables and interpretations for the SPR MACs. A summary of this process is presented in Roberts, 2021 [10]. In brief, this procedure takes the uncorrected LAS radial arm data and computes several summary values at each depth station. These provide information on the casing geometry and deformation level as a function of depth. One of these summary values, the coefficient of variation of the diameter values (Cv) is used in the discussions below. The Cv values show how the diameter values in a casing cross-section vary; larger Cv values indicate greater casing deformation. The MAC analysis procedure also computes the minimum diameter values which are useful in understanding how much any deformation impacts well operations. A decrease in minimum diameter can prevent the use of logging tools in the well and impact other well operations.

3.3.1. General MAC Discussion

MAC logs were first collected at the Big Hill SPR site in 2010. Since then, there have been at least two MAC surveys collected from each well. Table 3-1 presents the time range and total count for MAC surveys at each of the Big Hill wells. Also shown in this table are estimates of the Minimum Diameter change Rate and the Expected Year of severe Deformation.

The Minimum diameter change rate column in Table 3-1 presents a best estimate, when possible, of the most representative value of change in the minimum diameter of the inner-most cemented casing at the salt-caprock interface. This is given in inches per year. In many cases, there is insufficient information (MAC surveys) or deformation levels are too small to compute a meaningful rate.

There are many factors that can add uncertainty to the minimum diameter rate calculations, the greatest being the nonlinear nature of the deformation. As the casing is deformed it loses strength which allows it

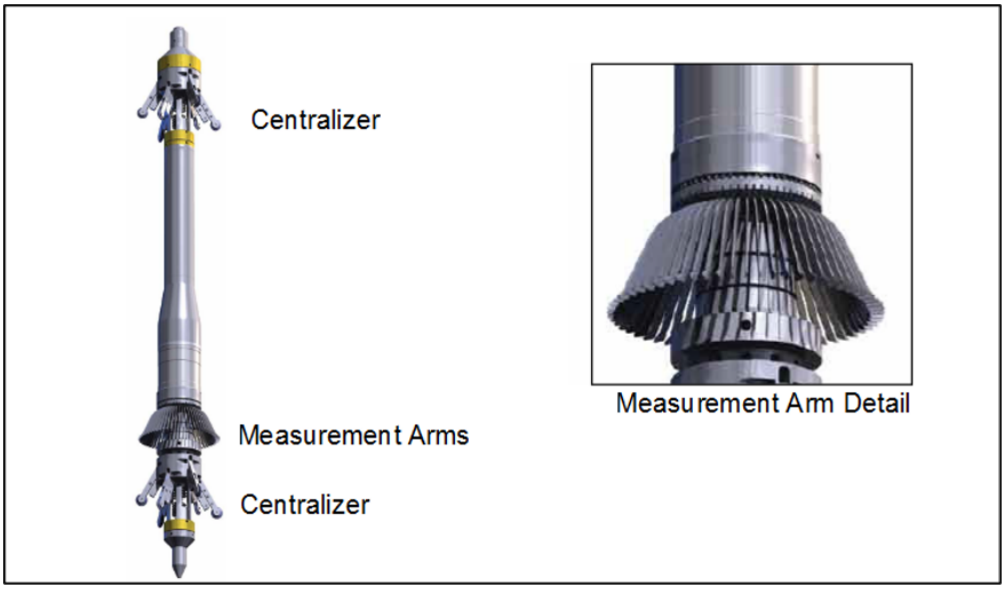

Figure 3-7. Weatherford 60-arm MAC tool

to deform at an increasing rate. So, in most cases, minimum diameter change rates computed from the existing data likely underestimate future rates.

The "Estimated year of severe deformation" column provides an estimate of when the well's minimum diameter will decrease by one inch from its original configuration. For this report, this level of deformation is considered severe enough that the well would likely need to be abandoned at that point. This date is computed from the minimum diameter change rate and so it is affected by the same uncertainties as that value. Note that this date only addresses casing deformation and not loss of well pressure integrity.

Based on the minimum diameter change rates shown in Table 3-1, the well most likely to experience severe deformation the soonest is BH-114A (2030) followed closely by BH-109B (2034). All the other active wells are not expected to reach a severe level of deformation for at least another 20 years. Two wells, BH-106B and BH-107B don't have sufficient information to compute a meaningful minimum diameter change rate and so predictive estimates can be made for them. BH-106B has had a liner installed in the well but has not had a subsequent MAC survey. Prior to liner installation, this well was showing signs of extreme casing deformation, so this well is expected to continue experiencing deformation into the future. Similar to BH-106B, BH-107B was showing signs of significant deformation and then was lined. A single MAC log was run on the liner in 2023 (five years after liner installation) and at that time, the liner did not show significant signs of deformation. Given the history of this well and the good condition of the liner, it is expected that this well will not experience severe deformation for many years. As a reminder, the severe level of deformation is the point at which the well is no longer useable and would likely need to be abandoned.

3.3.2. CV Mapping

As discussed above, the computed Cv value is used as a measure of casing deformation; larger Cv values indicate greater deformation. The following discussion presents an analysis of the spatial pattern of casing

Table 3-1. Orientation of minimum diameter at maximum Cv depth.

Well	Install Date	Earliest MAC	Latest MAC	MAC Count	MD Rate (in/yr)	Ex Deform Year
BH-101A	01/08/85	07/20/10	07/23/20	2	A*	A*
BH-101B	10/25/84	10/30/12	01/13/22	2	A*	A*
BH-102A	09/21/84	08/24/10	09/09/20	2	0.014	2085
BH-102B	11/30/84	05/10/12	12/14/21	2	A*	A*
BH-103A	09/04/84	07/21/10	01/03/19	5	A*	A*
BH-103B	11/09/84	04/11/12	10/03/18	3	0.013	2092
BH-104A	10/08/84	06/28/10	07/06/23	4	0.025	2049
BH-104B	02/12/85	01/04/13	07/25/23	3	0.033	2047
BH-105A	09/17/84	05/25/10	10/29/20	4	A*	A*
BH-105B	12/03/84	06/09/10	02/14/23	7	C*	C*
BH-106A	02/02/84	10/27/10	01/12/23	4	A*	A*
BH-106B	11/21/83	12/03/12	12/21/22	3	B*	B*
BH-107A	11/18/83	09/07/10	01/11/23	4	0.008	2146
BH-107B	02/01/84	11/08/12	01/26/23	3	B*	B*
BH-108A	10/23/83	07/13/10	01/21/15	2	0.01	2105
BH-108B	01/03/84	10/22/12	01/11/21	3	A*	A*
BH-109A	09/09/83	06/29/10	04/06/23	3	0.016	2066
BH-109B	11/27/83	01/31/11	04/05/23	4	0.046	2034
BH-110A	09/19/83	06/23/10	05/13/20	2	A*	A*
BH-110B	11/23/83	06/07/12	11/22/16	2	A*	A*
BH-111A	02/19/85	09/08/10	03/27/23	4	0.009	2123
BH-111B	04/24/85	08/23/12	02/28/23	4	A*	A*
BH-112A	05/06/85	09/09/10	08/18/21	4	A*	A*
BH-112B	02/25/85	07/31/12	11/23/21	3	A*	A*
BH-113A	06/26/85	08/26/10	08/19/21	5	0.026	2053
BH-113B	04/17/85	07/02/12	05/04/23	3	B*	B*
BH-114A	08/04/85	07/14/10	09/23/23	5	0.06	2030
BH-114B	04/14/85	03/22/12	02/10/22	3	0.015	2084

deformation as represented by maximum well lifetime Cv values. These Cv values are the maximum Cv seen in the area of the salt-caprock interface from any MAC survey conducted during the lifetime of the well. This would include MAC survey on remedial liners as well as the original casing.

In the graphics shown in Figure 3-8, the individual maximum Cv values have been spatially interpolated to provide easier visual interpretation. The values between the wells are only estimations and their uncertainty increases with increasing distance from the well locations. The interpolations are strictly intended to help determine potential spatial patterns and are not necessarily predictive.

The upper plot in Figure 3-8 shows the maximum Cv values interpolated across the region of the storage cavern field. In this figure, the highest maximum Cv values are shown in dark red and the lowest are shown in green. The color scale bar represents a linear progression from highest to lowest Cv values. Several of the cavern well pairs have greatly differing maximum Cv values which can be seen as separate "bullseye" patterns around the individual wells for a given cavern. The obvious examples are caverns 105 and 114.

The general pattern in the plot of Figure 3-8 shows the highest deformation region on the western end of

the site with two high deformation areas on that end separated by a lower deformation area in between. The general observation of higher deformation on the western side is confounded by the very low deformation seen at both wells for cavern BH-110 which is the western most cavern. The wells in the eastern 60% of the site show much lower levels of deformation with the southern section of this region having slightly higher values than the northern section.

The lower plot in Figure 3-8 shows the interpolated Cv data with an overlay displaying the locations of shear zones in the salt and caprock as well as top of caprock faults as mapped by Rautman et al. [8]. The shear zones represent the boundary between different salt spines. Salt spines are regions of the salt dome that may move independently of one another. The salt spines are interpreted from structural contours of the salt and caprock. A valley in the top structural contours is interpreted to be the margin of a salt spine; valleys in the top of caprock contours are also interpreted as related to salt spines since the caprock is a product of salt dome rise. Both sets of interpreted spine margins are shown for completeness.

In general, there does not appear to be a consistent relationship between the location of the salt spine boundaries and areas of high and low well deformation. The north-eastern portion of the site has the highest density of salt spine margins yet has some of the lowest levels of deformation. Although there are examples of extreme deformation right at a salt spine margin, specifically BH-114A, its well pair, BH-114B shows much lower deformation even though it falls within the same mapped spine margin. In addition, the well with the greatest level of deformation, BH-105B, is distant from the spine margins. There is a top-of-caprock fault mapped between the BH-105 well pairs. This fault is based on a difference in caprock top elevation between the A and B wells, but this difference is not seen at the top-of-salt so the fault's vertical extent may be limited to the upper portion of the caprock. The northwest corner and south-central regions of the site fall between salt margins. Unfortunately, these regions also do not offer a set of consistent observations. Although the southern section does show relatively low casing deformation, the north-western section shows both very high and very low deformation levels.

The search for an explanation for the spatial pattern of well deformation as represented by Cv value offers mixed results. Although there is some general agreement between geologic features (shear zones and caprock faults) and the gross pattern of Cv values, there are also much inconsistency between the two. This inconsistency prevents a full reckoning between the geologic features and known casing deformation, with the mapped geologic features offering no real predictive power for Cv value.

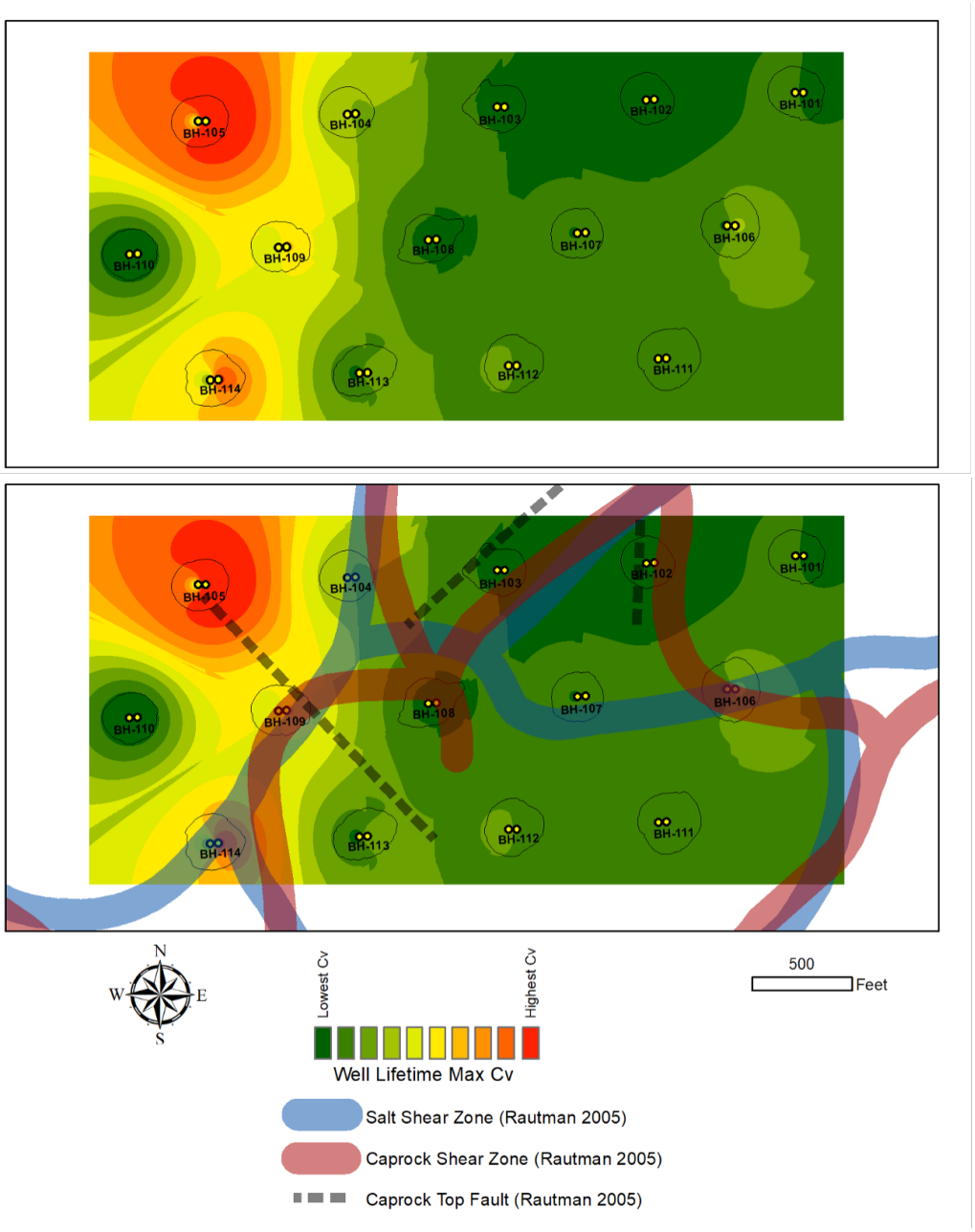

Figure 3-8. Interpolated Big Hill lifetime maximum Cv values (top) with salt spine boundaries from salt (blue) and caprock (red) structures in bottom plot. Spines after Rautman et al. 2005.

3.3.3. CV Over Time

Another way to examine the CV value is looking at the CV over time. Figure 3-9 shows the maximum Cv value at the salt-caprock interface for each of the Big Hill wells in the form of a sparkline. A sparkline figure was chosen as the best method to compare and contrast Cv values *through time*. All of the figures show the same timeframe on the x-axis and the all of the y-axes show CV values between 0 and 0.05 (not shown on the figure for readability). The orange lines lines represent the "A" wells and the blue lines repesent data from the "B" wells. Additionally, lined wells are represented with black outline around the point.

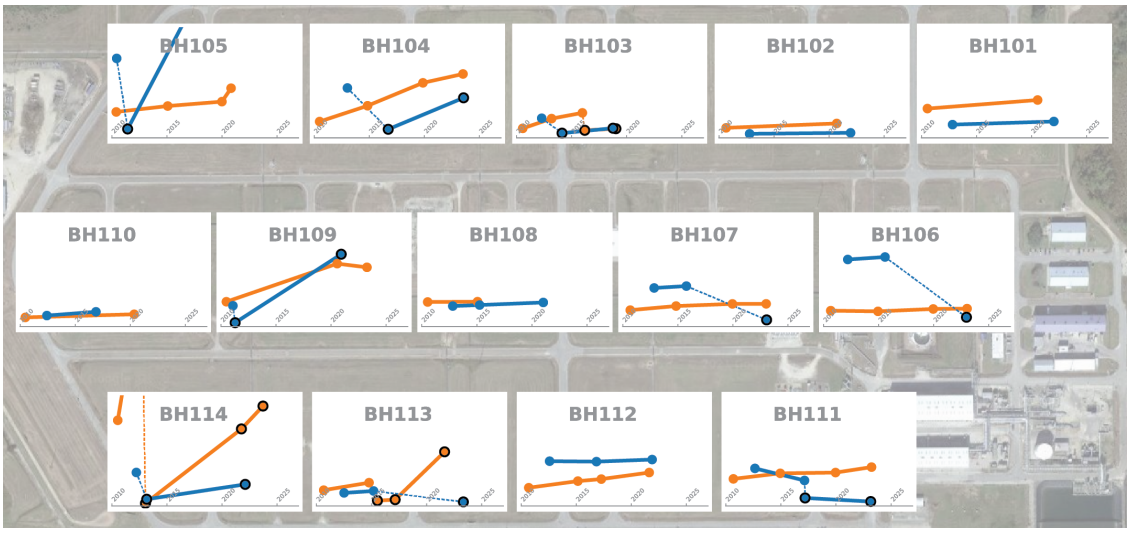

Figure 3-9. Maximum Cv value at the salt-caprock interface for each well at Big Hill that represents the out-of-roundness (higher Cv values mean greater out-of-roundness). The orange values show the A wells while the blue shows the B wells. Lined wells are shown with a black outline on the point. Dashed lines show the time between an unlined MAC survey and a lined survey.

Information in Figure 3-9, shows that most of the wells have a maximum Cv value that is increasing over time; however, the rate of change varies significantly between wells. As previously established from the information in Figure 3-8, wells in BH-105, BH-109, and BH-114 have higher CV values. Of those three caverns, only BH-109 is showing consistent deformation rates in both the A and B well. In caverns BH-105 and BH-114, the deformation rates are higher in either the A or B well. In BH-109, the B well is experiencing a large amount of deformation while the A well has relatively stable deformation since 2010. There is a slight increase in deformation in BH-105A near the end of the observed time. It is undetermined whether BH-105A will continue to increase at the increased rate. BH-114 has the highest deformation in the A well (which is in contrast to BH-105). BH-114A was lined in the early 2010's but has continued to increase ever since. The B well was lined around the same time and has also continued to increase, but at a much lower rate.

All of the wells on the eastern part of the site show little to no increase in their CV values over time. In addition to the eastern wells, the wells at BH-110 seem unaffected at the salt-caprock incerface. The CV values in both wells have consistently been the lowest at Big Hill. BH-110 seems to be isolated from the phenomena is impacting the adjacent wells.

3.3.4. *Orientation of Deformation*

Since late 2021, the MAC logs at the Big Hill site have been run with a gyroscopic orientation tool which provides absolute orientation of the logging data. This information can then be used to orient the radial deformation seen in the MAC data. When sufficient deformation is evident, it is possible to use the orientation of the minimum diameter vector to estimate the orientation of the maximum stress acting on the innermost casing. The thought being that the direction of maximum geologic stress is parallel to the minimum diameter direction. This process can be applied to each oriented MAC data set and the resulting collection of orientation vectors used to investigate any spatial patterns in the casing deformation.

The results from this type of analysis are shown in Figure 3-10 below. The red arrows indicate the direction of maximum stress acting on the innermost casing as represented by the minimum diameter. The depth for the minimum diameter location is taken as the depth with the maximum Cv value. Wells with oriented MAC data which does not have sufficient deformation to make a meaning orientation determination are shown by the yellow circle and are listed as 'indeterminate'. Wells which currently do not have oriented MAC data are shown by black dots without any orientation indicator.

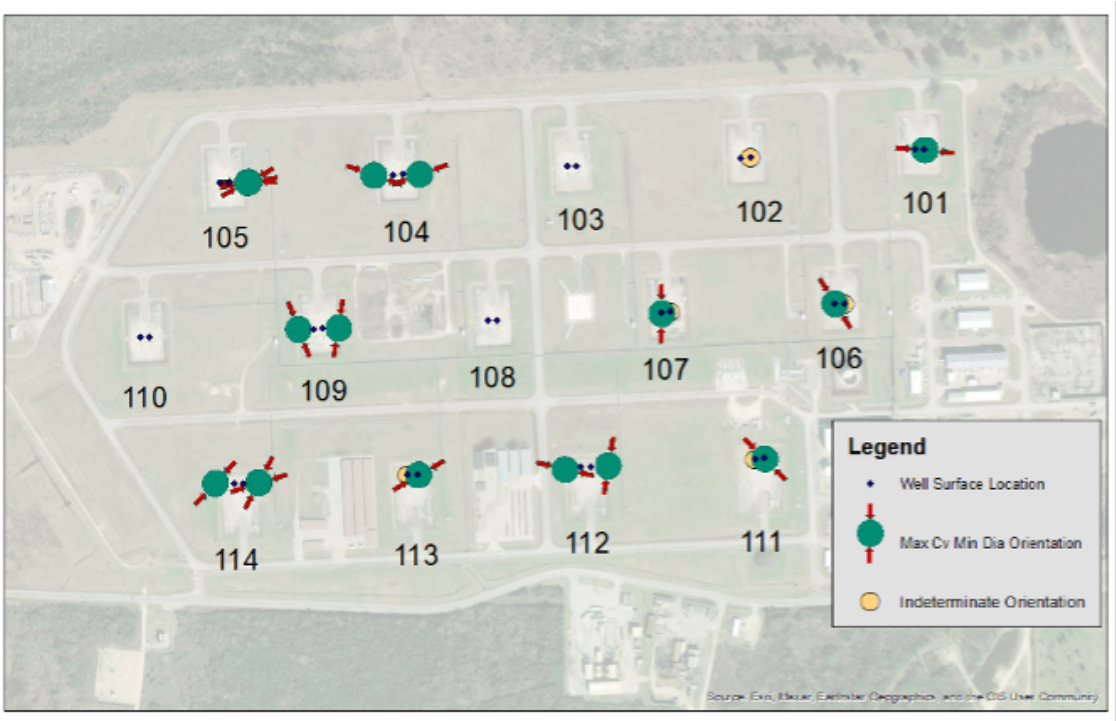

Figure 3-10. Orientation of minimum diameter at maximum Cv depth.

As shown by Figure 3-10, there is no single, determinant pattern of the direction of maximum stress. The northern most row of wells does show some preferred east-west orientation, but this is contradicted by the middle row of wells which show a preferred north-south orientation. The southern-most row of wells shows a mixture of orientations. It is possible that the middle row of wells reflect a differing stress-regime than the northern in southern rows since it is flanked on either side by other wells. This explanation seems less likely when one considers the relatively small diameter of the well bores compared to the relatively large distances between cavern well pads. It seems more likely that the changes in orientation of maximum

stress reflect small-scale changes in the factors leading to casing deformation across the site. This idea is also supported by locations where well pairs show differing levels and orientation of deformation. There are four caverns (BH-106, BH-107, BH-111, and BH-113) whose well pairs show significantly differing levels of deformation as shown by one of the wells having an indeterminate deformation orientation. And one cavern (BH-112) with well pairs having deformation orientations perpendicular to one-another. In summary, although the oriented MAC data provide valuable information regarding the deformation dynamics for a single well, the small-scale variability in these dynamics, as evidenced by the variability in the deformation orientations, mean no cavern-field wide interpretation is possible from this data.

3.3.5. Caverns Expected to Provide Reliable Storage into the future (2055)

One of the goals of this report is to provide guidance on which Big Hill storage caverns can be expected to provide reliable storage into the foreseeable future. For this discussion, the foreseeable future is defined as extending to the year 2055, approximately 30 years from the date of this report. Here reliable storage is defined as the ability to move oil in and out of the cavern using a two-well system as initially designed. As such, this ability is most dependent on the reliability of the cavern access wells. Potential cavern issues such as cavern-to-cavern communication and cavern diameter growth are not considered here. This section covers expectations based on the analysis of MAC logging data focusing on minimum diameter rate values (Table 3-1) and the spatial distribution of maximum Cv values (Figure 3-8). These two parameters were chosen because they offer the greatest potential to inform on the future storage reliability of individual caverns.

An examination of the minimum diameter change rates listed in Table 3-1 and the maximum value Cv mapping in Figure 3-8 shows that there are nine Big Hill caverns that should provide reliable storage at least until the year 2055. These caverns are listed in Table 3-2.

Table 3-2. Caverns expected to provide reliable storage till at least 2055

Caverns
BH-101
BH-102
BH-103
BH-104
BH-107
BH-108
BH-110
BH-111
BH-112

The caverns listed in Table 3-2 were selected, in-part, based on their projected date for extreme deformation based on the computed minimum diameter change rates. In some cases, no change rate was available in which case an examination of the MAC history of the well was used to assist in the decision. The other factor considered in assembling the list in Table 3-2 was the spatial distribution of maximum Cv values. During this, the general pattern of the maximum Cv values, the relationship to adjacent caverns, and the

general well histories were all considered. It is also noted that the minimum diameter change rate and maximum Cv values are not fully independent and do share some correlation.

These expectations for reliable storage are based strictly on projected well reliability based on MAC logging history. Many other unknown factors will also determine the actual future reliability of these caverns.

3.4. Surface Deformation

Surface deformation is another metric we can use to try and understand well deformation at the site. Traditionally, it has been used to monitor cavern integrity but surface deformation may also be impacted by the same phenomenon that is impacting well deformation.

Surface deformation at Big Hill has consistently been some of the highest in the SPR. Historically, the highest subsidence at Big Hill has been just under 1 in./yr. Recently, subsidence has increased slightly with the highest deformation still near the center of the cavern field. The primary method of measuring surface deformation is InSAR, or Interferometric Synthetic Aperture Radar. InSAR is a satellite-based technique that is able to measure vertical deformation on the submillimetric scale. The SPR has used TRE Altamira as the primary provider for InSAR since 2017. Figures 3-11-3-13 are from the most recent report from TRE Altamira [11].

3.4.1. 1D InSAR Data (Ascending & Descending)

Figure 3-11 shows the two types of data the SPR receives from TRE Altamira - ascending and descending data. Ascending and descending datasets refer to the orbits of the InSAR satellite. Ascending data is when the satellite observes the site in an south-to-north orbit and the descending data is a north-to-south orbit. In each of the orbits view the site from different angles and are eventually used to calculate 2D datasets. The ascending data viewed the site from the west (eastward looking) at a 17.8°from azimuth. Ascending data is looking almost directly down at the site. The descending data viewed the site from the east (westward looking). The descending data was taken at a more oblique angle at 54.6°.

Figure 3-11 shows the Area of Interest (AOI) and the reference point shown as a black dot in the NE part of the figure. Additionally, the salt dome footprint is represented as a light gray outline in the figure. The most striking difference between the two orbits is the amount of spatial coverage. The ascending data has great coverage over the entire AOI while the descending data is only reflecting off of the roads and site infrastructure. This will impact the coverage of the 2D results. Data from both orbits are necessary to calculate 2D results at any given location.

The ascending data in Figure 3-11 shows that subsidence extends beyond the cavern field and into the northern part of the salt dome. For many years, we thought that Big Hill was uplifting. After the implementation of InSAR, we were able to see that Big Hill was not, in fact, uplifting. Rather, the reference monument was subsiding faster than parts of the site. That monument was located north of the site on the other site of the forested area adjacent to the site.

The ascending data shows that, although the highest subsidence is near the center of the cavern field, the area of subsidence extends preferentially to the north, within the footprint of the salt dome. In other words, the area of subsidence stays largely within the foot print of the salt dome. As mentioned in Section

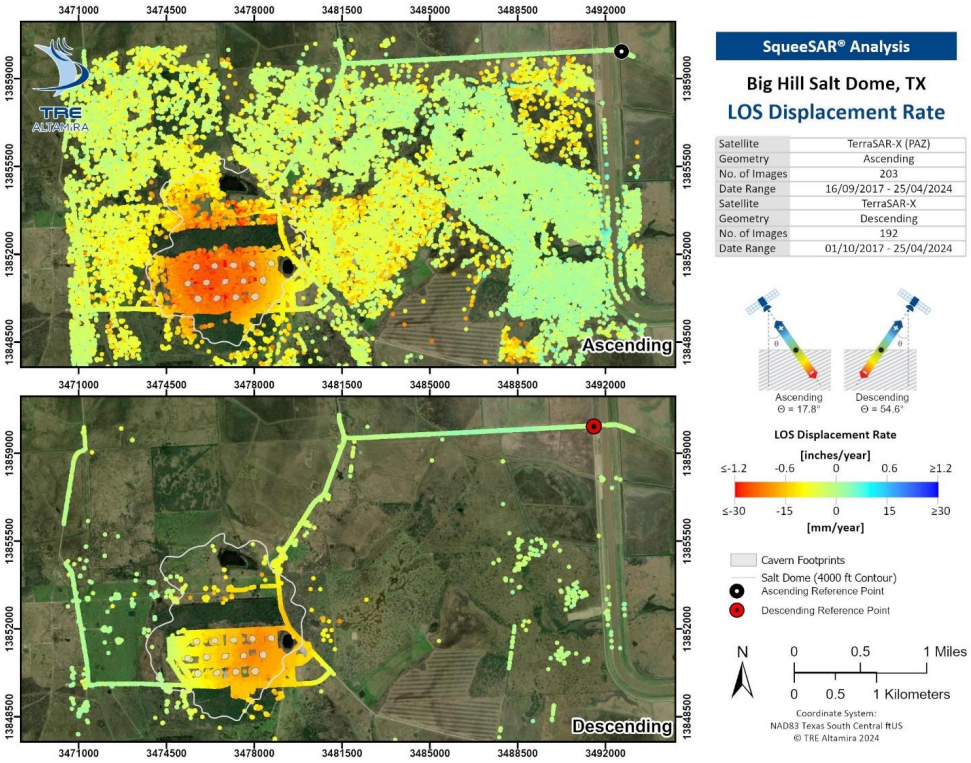

Figure 3-11. Ascending and descending LOS SqueeSAR annual displacement rate (September 2017 - April 2024). From TRE Altamira report.

3.2, Big Hill has a thick caprock. One theory for the deformation at the salt-caprock interface suggests that rising salt spines cannot push the resisting force of the massive caprock and is pushing laterally outwards thus creating shear forces at the salt-caprock interface. The thick caprock may also influence the pattern of subsidence at Big Hill. As caverns close, the deformation eventually expresses itself at the surface - typically subsidence. The rigid nature of the caprock may influence how cavern closure is expressed at the surface. In this case, it may spread the area of subsidence over a larger area of the dome. This would also explain the subsidence being largely confined to the area above the caprock.

One confounding counter-point to this theory is that we see a subsidence bowl centered over the cavern field. This suggests stresses are being expressed through the caprock and up to the surface - indicating the thick caprock is not completely rigid. If the caprock were completely rigid, we would expect to see more uniform subsidence across the dome, not the subsidence bowl that we see in the results. We know there are faults in the caprock which could play a role in how stresses are translated to the surface. These faults may also play a role in the movement at the salt-caprock interface; however, there is no site-wide correlation between subsidence and well deformation. Additionally, well deformation can be highly localized while subsidence is a regional effect spread across the dome footprint. As such, subsidence is not a good indicator of well deformation at Big Hill

3.4.2. 2D InSAR Data (Vertical & Horizontal E-W)

Figure 3-12 shows the vertical and horizontal east-west deformation calculated by TRE Altamira. As previously mentioned, the spatial coverage of the 2D measurements are largely determined by the spatial coverage of the descending data. This means that most of the results are limited to the roadways and site infrastructure. Outside of the site, there is little surface deformation but inside the site, the vertical deformation shows a bowl-like subsidence over the cavern field.

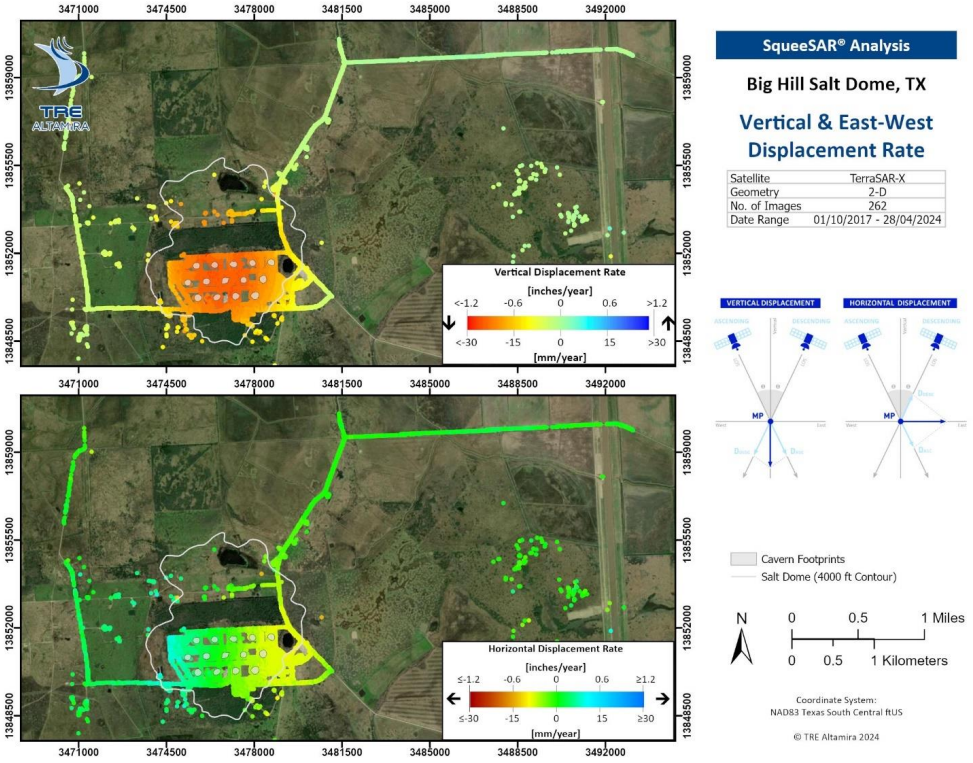

Figure 3-12. Vertical and East-West annual displacement rate (October 2017 - April 2024). From TRE Altamira report.

Figure 3-13 shows a closer view of the 2D InSAR results. The 2D vertical shows higher subsidence in the center of the site as represented by the warmer colors. The 2D horizontal E-W data shows the horizontal movement in the east-west direction. There is no north-south component due to the orientation of the satellite orbit. The 2D horizontal data shows that most of the site is experiencing little to no horizontal movement - except for the eastern and western edges of the site which show movement towards the center of the site. The western part of the site is moving eastward and the eastern part of the site is moving westward. There is likely some north-south component to the movement but, currently, there is no way of measuring this with InSAR.

Until 2021, West Hackberry had the highest subsidence. In 2021, subsidence rates at both Big Hill and West Hackberry increased and began to decrease in 2022. The median elevation change over time has been steady since the beginning of 2023. One thing unique to Big Hill is the difference in subsidence rates across the site (i.e. the value between the 10th and 90th percentile is much larger than the other three sites).

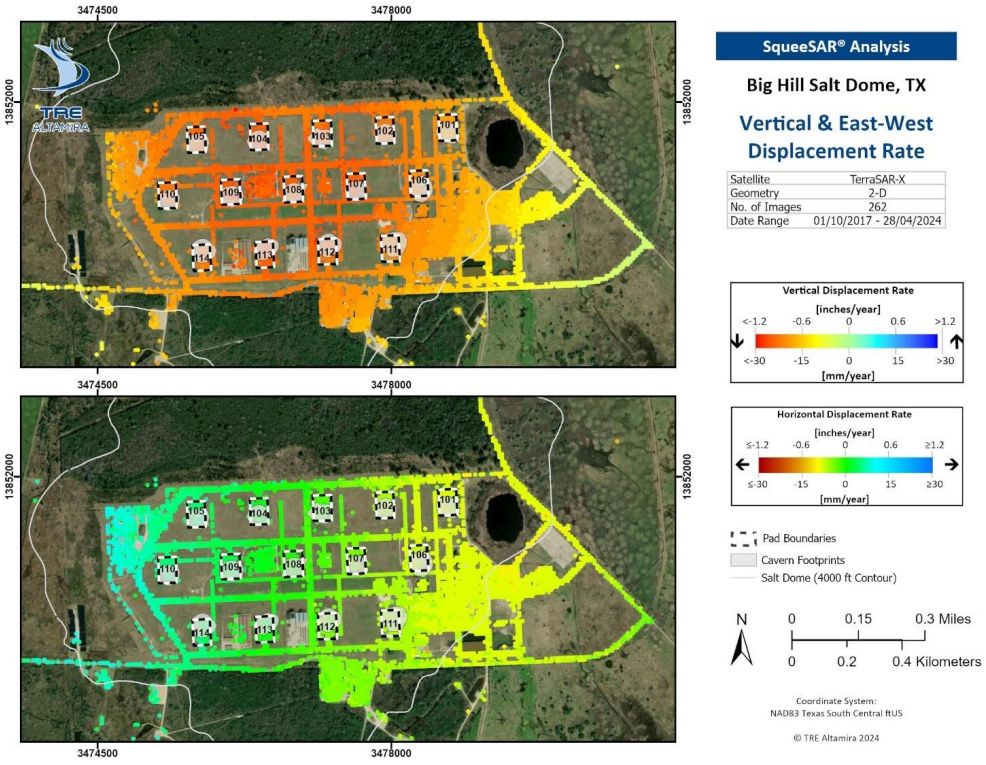

Figure 3-13. Vertical and East-West Displacement Rates over the Storage Facility. From TRE Altamira report.

This could be because the easternmost part of the site is experiencing far less subsidence than the rest of the site.

According to the average subsidence rates calculated by TRE Altamira, most of the wellpads are experiencing subsidence rates around one inch per year. The area above Caverns BH-104, BH-107, BH-108, and BH-109 are experiencing downward movement slightly more than one inch per year. This is expected as these caverns are nearest to the middle of the cavern field and at the bottom of the subsidence bowl.

3.4.3. Summary of Surface Deformation

Although Big Hill is experiencing some of the highest subsidence at any of the SPR sites, there is no indication any of the caverns have been structurally compromised. Big Hill caverns have the benefit of being far below a thick caprock and adequately spaced far enough from any other caverns. The biggest concern at Big Hill is the structural integrity of the wells at the salt-caprock interface. There are several wells that have become unusable due to the amount of deformation in the well. Unfortunately, surface deformations do not seem to be a good indicator of where well deformation will occur or how fast it will occur.

3.5. Comprehensive Monitoring

3.5.1. Comparing Oil Transfers to Subsidence Rates

Two sites, West Hackberry and Big Hill, both showed changes in subsidence around the same time — which is also around the time of the oil sales. As such, the first approach is to determine if changes in site operations may have contributed to the change in subsidence. At a high level, we want to see whether or not surface velocities change with a change in site operations. This is easier said than done. Although InSAR is accurate and numerous, we are measuring data from a real-world system that can be noisy. We cannot *directly* derive any meaningful velocity from the InSAR data because any noise in the position data will be exacerbated in the corresponding velocity data. Instead, we will need to smooth the InSAR data to approximate surface velocities across the site.

We can smooth the InSAR data using a localized regression method called LOWESS. LOWESS, or **Lo**cally **We**ighted **S**catterplot **S**moothing, is a non-parametric smoothing function that relies on least squares fitting on local regions within the dataset (i.e. it performs a linear estimation on each section of the data to determine the best fit). The best way to characterize the site with a single dataset is with the median subsidence data already presented in Figure 1-1. This dataset was used to perform the LOWESS smoothing. A window of 1/13 of the dataset (approximately six months) was used for the regression. Results from the smoothing algorithm are shown in Figure 3-14. The smoothed data are laid on top of the original displacement data. Because of the LOWESS process, the first six months and last six months of the smoothed data may not accurately represent the original data.

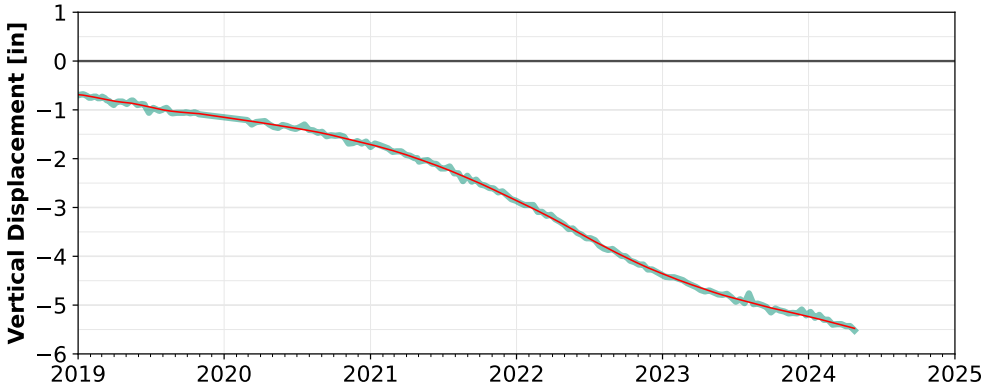

Figure 3-14. Median surface deformation across the Big Hill SPR site shown in purple with LOWESS smoothing estimation overlaid in red.

Velocity data were subsequently calculated using the smoothed data. The gradient of the smoothed displacement data was calculated using a central difference method. Resulting velocity data are shown in Figure 3-15.

While there are many site operations to compare (e.g. oil/brine transfers into or out of caverns, cavern pressures, etc.) site oil transfers out of the caverns by month will serve as a proxy to estimate site operations as a whole. The visual comparison between the monthly oil transfers and the velocity profile is shown in Figure 3-16. The two curves share the same x-axis (time) but the y-axes measure different quantities. The y-axis to the left of the figure in black corresponds to the monthly oil transfers out of the Big Hill

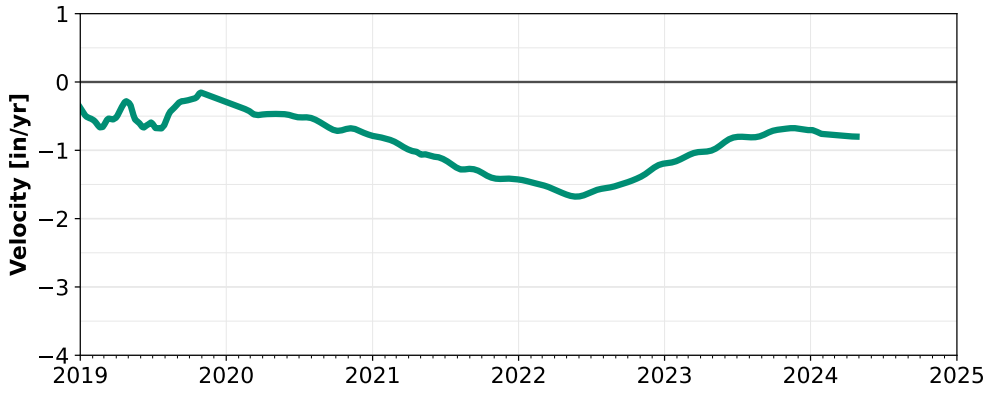

Figure 3-15. Median Big Hill surface velocity derived from LOWESS smoothing

caverns. The y-axis to the right of the figure shows the surface velocity calculated in Figure 3-15 but this time inverted and scaled.

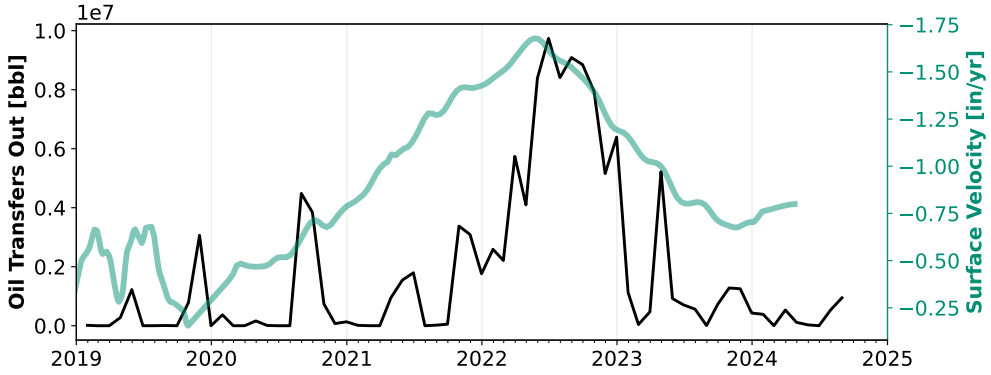

Figure 3-16. Qualitative comparison between oil transfers out (black) and median Big Hill surface velocity (teal).

Qualitatively, the two curves share a similar shape at corresponding points in time. This may suggest that there is a correlation between oil transfers and increased subsidence at the site; however, there are several other factors that must be considered:

Correlation ≠ Causation. It is important to remember that correlation does not equal causation. Just because the two quantities may be correlated in time, one might not cause the other. For example, oil transfers alone should not impact subsidence. It is likely that reduced cavern pressures during fluid transfers increase cavern creep and, in turn, increase deformation at the surface.

Site Level Comparison. This comparison was completed at the site level – meaning the information is in aggregate. It is possible that some areas of the site are more susceptible to changes in subsidence rates. It may be possible to analyze the data at cavern level but there are complications to this approach as well.

Not spatially dependent. Because the analysis is at the site level, there is no spatial component to the data. The analysis was completed by aggregating all the InSAR data within the SPR boundary

and then completing an analysis on that data. Although InSAR coverage is excellent at Big Hill, there is the possibility that aggregating the results may have biased the velocities to reflect areas with greater InSAR reflections. These would be areas that have permanent infrastructure like well pads or the control center in the middle of the site. In practical terms, places like grassy fields are more likely to be left out of the analysis because there are less InSAR reflections. An alternative method for obtaining a site-wide analysis would be to regularize the data. This could be done through a method like Kriging; however, the resulting aggregate analysis would be based on an estimate of displacement results (i.e. one step away from the original data). Both methods have pros and cons and it is difficult to say which better represents Big Hill. Ultimately, both methods use estimates and should be taken into account when observing the outcome.

Discrepancies Between Datasets. While it looks like there are correlations between the oil transfers and subsidence deformation, this does not hold true for the entire time. There is a period in 2020 and 2021 where subsidence rates were greater than average but there were few oil transfers during that time. It is possible the increased subsidence during that time resulted from depressurization due to work-overs or some unforeseen effect.

Correlations on a Physical System. While possible correlations suggest mechanisms that drive subsidence, we still do not fully understand the subsurface. For example, there may be a time delay between oil transfers and an increase in subsidence. Possible time delays between cause and effect make it more difficult to attribute. Future datasets may help detection of any time delays.

3.5.2. Big Hill Well Deformation

We also combined much of the data previously presented in the report to see if there were any visual correlations between geological features, well deformation, and surface deformation. Figures 3-17-3-21 show various quantities co-located on a map of Big Hill.

The first map presented in Figure 3-17 shows the location of salt spines, well deformation orientation, and a surface deformation. The salt spines are shown as blue lines on the map. Wells with directional MAC surveys are shown as white circles outlined in black. If the survey showed a clear direction of minimum well diameter, the orientation is represented with black arrows. Because of the relationship between the minimum diameter and stresses at the salt-caprock interface, the arrows also indicate the primary stress direction. Subsidence is represented by small dots on the map. Warmer colors represent higher subsidence rates.

The direction of minimum well diameter is not consistent across the site - there are only slight trends. The northern row of wells (BH-101, BH-104, & BH-105) have an east-west trend in the primary stress direction. The middle row (BH-106, BH-107, & BH-109) shows a primary stress direction in the north-south direction. The southern row seems more random, but the wells in caverns BH-113 and BH-114 seems to exhibit a NE-SW trend.

Figures 3-18-3-20 show subsets of the same information presented in Figure 3-17. These figures are presented for visual clarity.

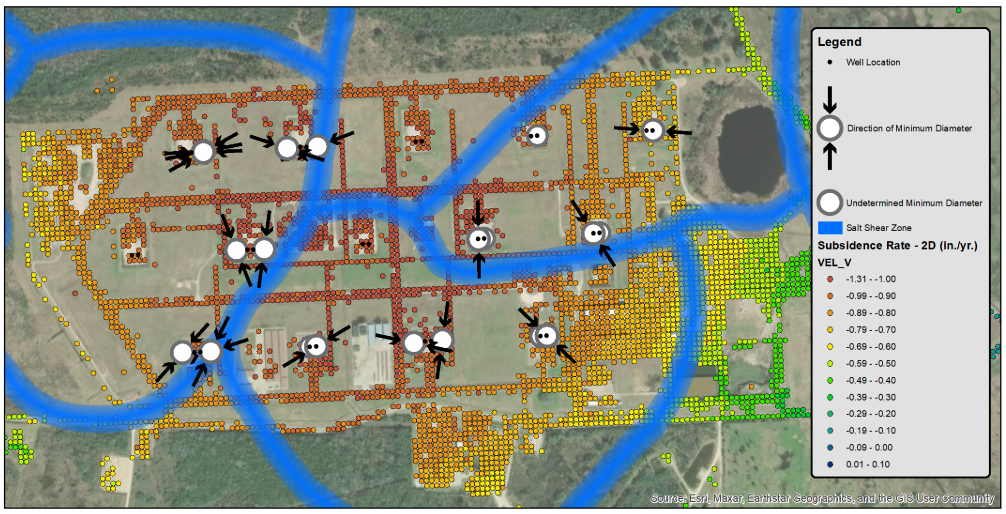

Figure 3-17. Comparison between salt shear zones, orientation of minimum well diameter at the salt-caprock interface, and subsidence rates at the Big Hill site.

Figure 3-18. Comparison between salt shear zones and the orientation of minimum well diameter at the salt-caprock interface at the Big Hill site

Figure 3-21 shows the location of the salt shear zones at the salt-caprock interface alongside the sparkline figures used in Figure 3-9. Most of the wells that show significant deformation over time seem to be along the NE-SW shear zone. The one exception is BH-105B which does not appear be near a shear zone.

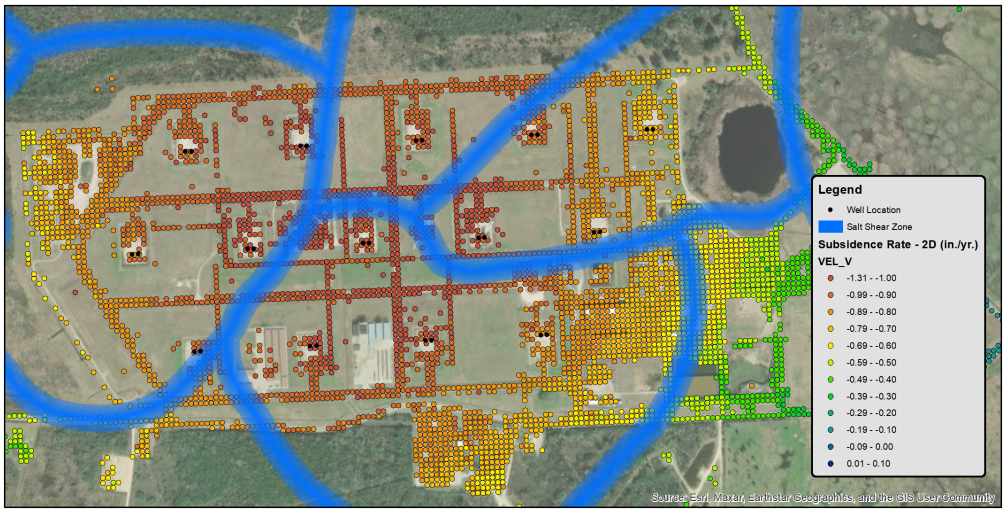

Figure 3-19. Comparison between salt shear zone and subsidence rates at the Big Hill site.

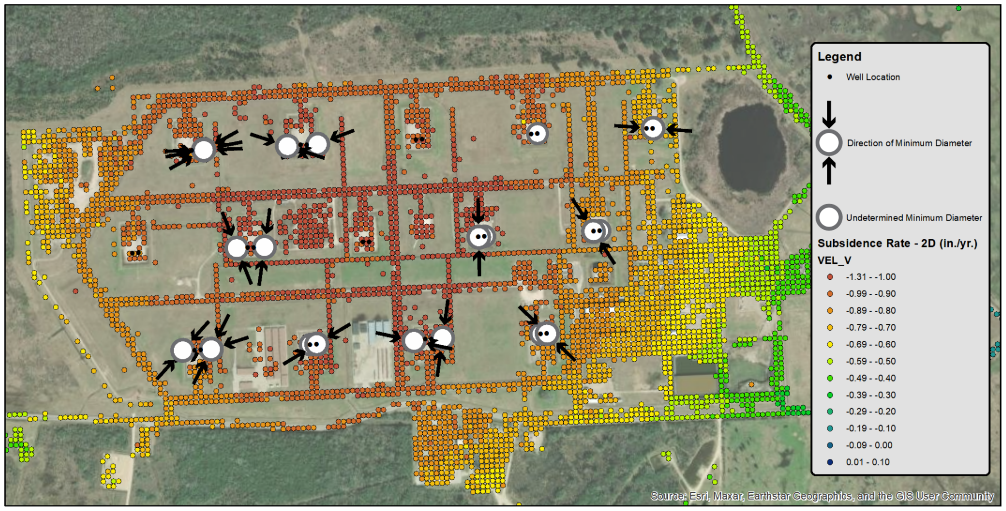

Figure 3-20. Comparison between the orientation of minimum well diameter at the salt-caprock interface and subsidence rates at the Big Hill site.

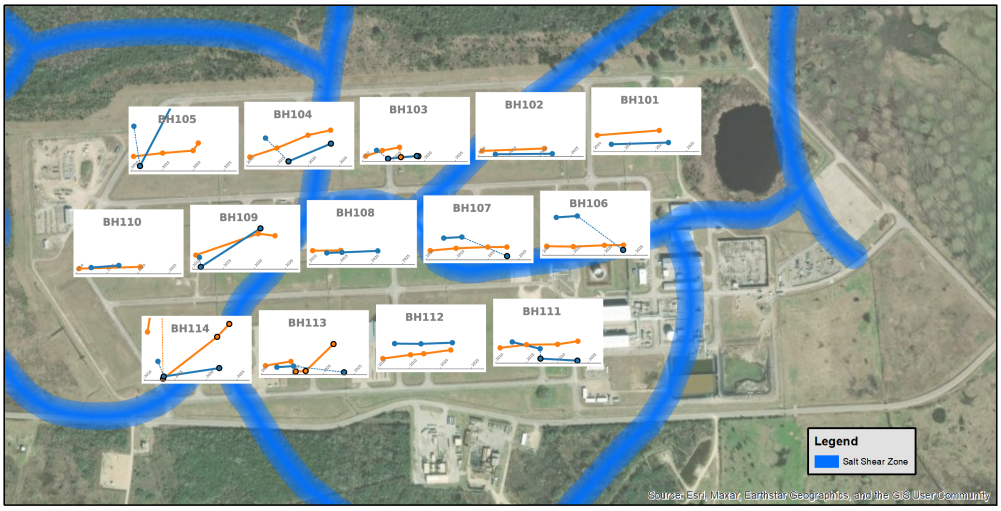

Figure 3-21. Comparison between salt shear zones and well deformation at the salt-caprock interface over time.

3.6. Big Hill Conclusions

Big Hill has proved to be one of the most difficult sites to predict. Subsidence rates have increased and subsequently decreased in the past 5 years and well deformation is being seen in more wells. This report presented a summary of our most current understanding of the geology, well deformation, and surface deformation at the site. We attempted to better understand the mechanisms that are impacting well deformation; however, there are only loose correlations that merely suggest at several possible causes. These correlations include:

- Directional correlations for some of the wells. Wells in the northern row of caverns have their minimum diameter oriented in the east-west direction. Wells in the middle row of caverns seem to have their minimum diameter oriented in a north-south direction. Wells in BH-113 and BH-114 also seem to have a NE-SW directional trend. These trends do not obviously correlate with any geologic features or subsidence rates at the site. It should also be noted some wells in these rows have not been measured using a directional MAC tool and may, or may not, follow the same pattern.
- Three caverns that are on one of the more active shear zones (BH-104, BH-109, and BH-114) are also experiencing some of the highest well deformations. It could suggest that the shear zone is influencing increases in well deformation. BH-105B is an exception to this. It is not near any known shear zone but is experiencing the greatest amount of well deformation at the site.
- There is a loose correlation between oil transfers at Big Hill and surface deformation. The greatest surface velocity at the site was seen slightly before the greatest oil transfer rates at the site; however, there are several factors (mentioned in Section 3.5.1) that should be considered before any conclusions are made.

Unfortunately, these loose correlations are not enough to suggest actionable steps to prevent further well deformation; however, we can say there is nothing to indicate that any of the caverns have become structurally compromised.

4. BRYAN MOUND

4.1. Introduction

Historically, Bryan Mound has had some of the most consistent surface deformation. Rates have been consistently linear with the highest rates above abandoned Caverns 003 (BM-003) and 002 (BM-002). This year is no different - the site-wide rates have not deviated significantly from historical rates. This year, however, BM-116A experienced a rapid depressurization that was caused by a well failure. Bryan Mound wells have experienced some axial well casing compression and, based on current information, it looks like BM-116A experienced a sudden axial compression. This report looks at the current surface deformation information to determine if there was an impact at the surface. Based on current InSAR, GPS, and tiltmeter information, there have not been any discernible impacts at the surface.

The monitoring program at Bryan Mound began in 1982 with annual level-and-rod surveys. In 2013, operators added a GPS and tiltmeter to supplement the level-and-rod data. Two more tiltmeters were also installed on the periphery of BM-003 but have since been decommissioned due to unreliability. Recently, the SPR has transitioned away from level-and-rod in favor of the satellite-based InSAR.

4.2. Surface Deformation

4.2.1. Interferometric Synthetic Aperture Radar (InSAR)

In 2016, Sandia decided to contract TRE Altamira to monitor Bryan Mound using InSAR. For the Bryan Mound surveys, the Cosmo-SkyMed (CSK) satellite was used. This particular satellite has a pixel resolution of 10 ft. x 10 ft. and a 16 day revisit time. The SPR has continuous InSAR data at Bryan Mound between October 2015 and July 2024; however, a subset of the data was taken this year to maximize the spatial coverage over the site [12]. This was done to prioritize viewing any events over BM-116A.

Bryan Mound is monitored using 2D InSAR measurements. This means that the site is measured from two different satellite orbits - ascending and descending. An ascending orbit means the satellite surveys the site with a south-to-north trajectory while a descending orbit has the satellite surveying the site using a north-to-south trajectory. An example of the 1D results is shown in Figure 4-1. Each orbit surveys the site from a different angle. TRE Altamira can use measurements from both orbits and calculate a 2D frame with true vertical and East-West horizontal surface movements at the site. Since 2D measurements require data from ascending and descending data we have 2D data beginning in October 2016.

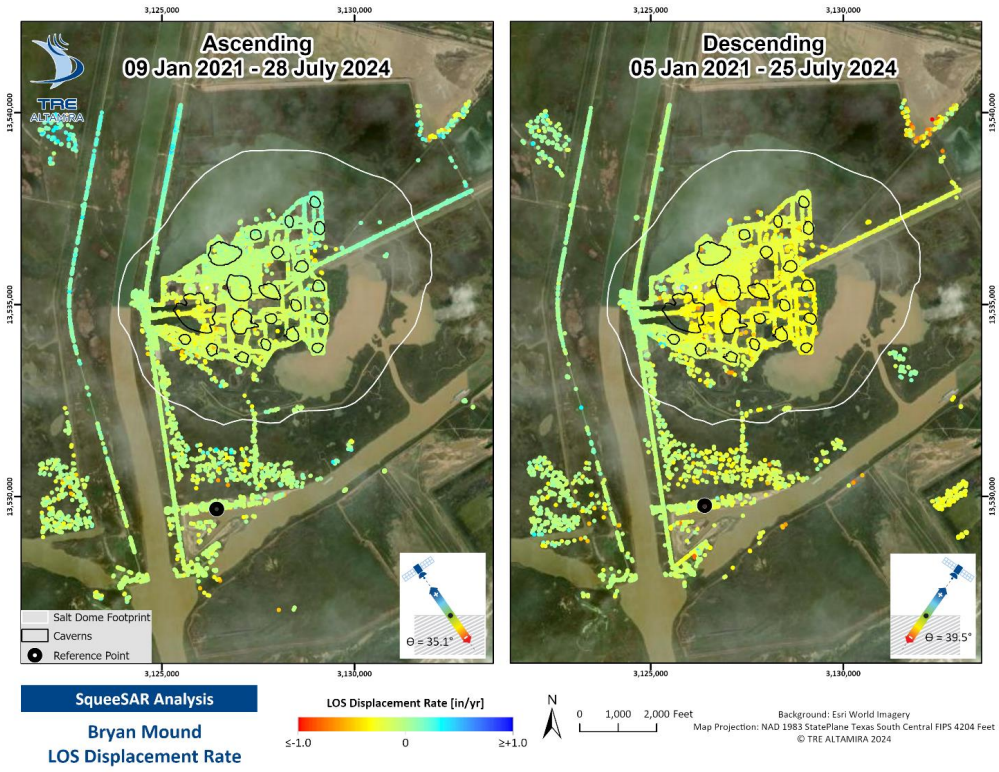

Figure 4-1. Ascending and Descending LOS SqueeSAR annual displacement rates above Bryan Mound (January 2021 - July 2024). *From TRE Altamira Report.*

Figure 4-2 shows the 2D vertical InSAR displacement rates between January 2021 and July 2024 while Figure 4-3 shows the horizontal rates for the same time period. Most of the vertical surface deformation is occurring above BM-003. The true vertical InSAR shows the greatest area of subsidence is over BM-003 and extends towards BM-002. The areas above BM-003 and BM-002 are subsiding at rates of -0.32 in./yr. and -0.25 in./yr., respectively. While most of the site is subsiding, the northeast area of the site is experiencing near zero movement.

The horizontal East-West results in Figure 4-3 shows most of the site exhibiting a slight westward deformation. It is important to remember that results from the horizontal 2D InSAR data only show the East-West components of displacement and do not show any North-South vectors. It is quite possible that there is some North-South component to the horizontal displacement but are unable to measure it with InSAR.

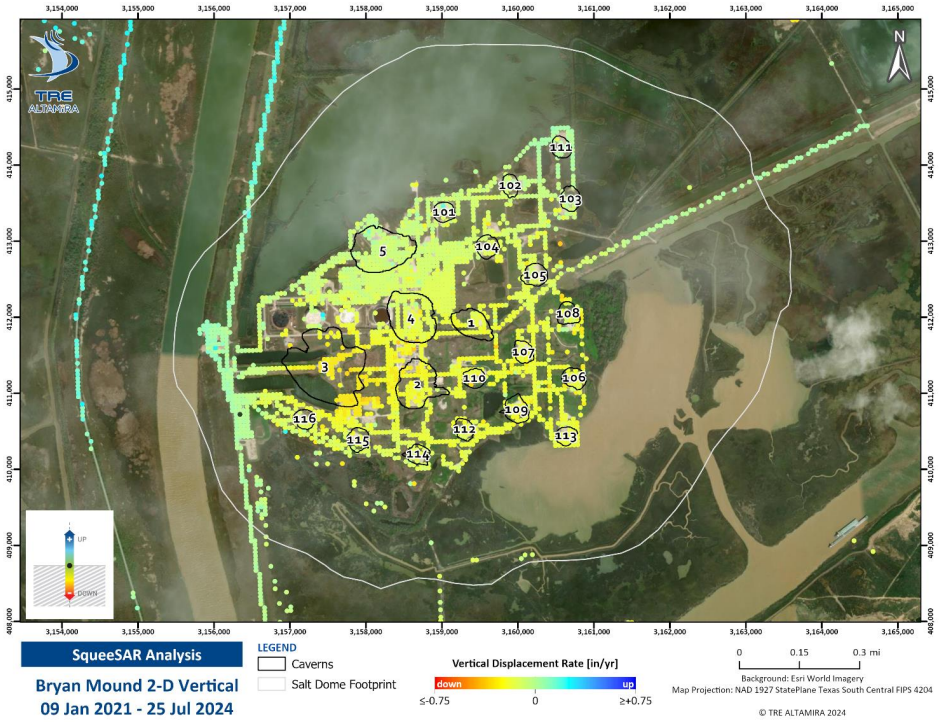

Figure 4-2. Annual vertical displacement rates over the Bryan Mound salt dome. ***From TRE Altamira Report.***

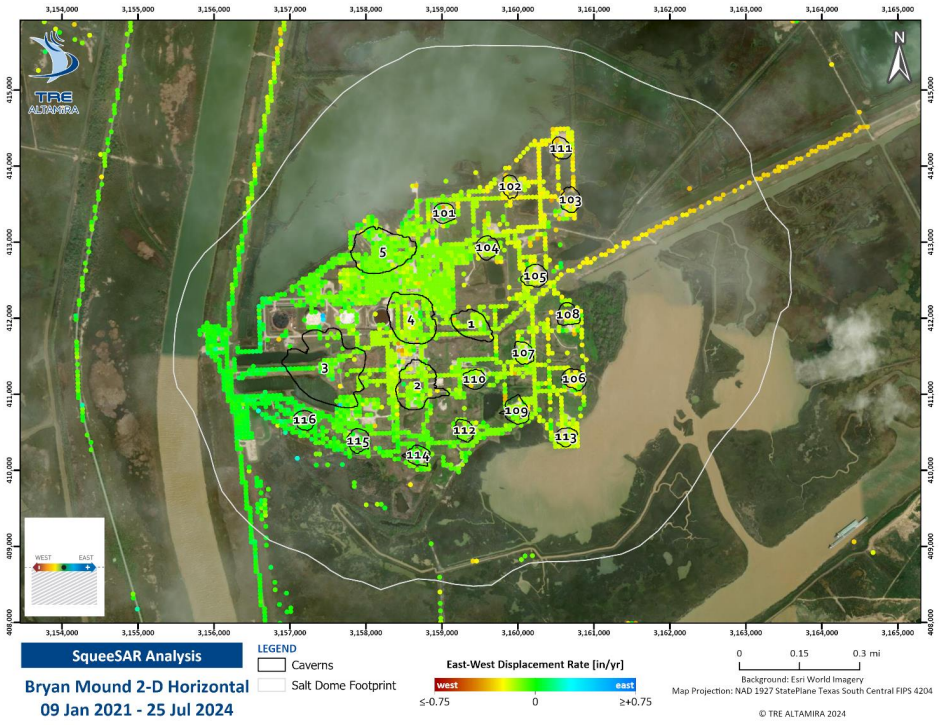

Figure 4-3. Horizontal (East-West) annual displacement rates over the salt dome. ***From TRE Altamira Report.***

4.2.2. *Realtime Sensing Instruments*

In the early 2010's SPR decided to supplement level-and-rod data with real-time sensing instruments over caverns of concern. As mentioned in the previous section, the cavern of highest concern at Bryan Mound is BM-003. The last sonar of the cavern in 1979 revealed a flat-shaped cavern with several petals branching away from the center of the cavern. After the sonar, the well was plugged and abandoned. There is no access to the cavern and the only way to infer the health of the cavern is through surface deformations.

4.2.2.1. GPS

There is a single GPS unit that was installed above BM-003 in early 2013. The GPS data in Figure 4-4 shows a linear subsidence rate of 0.30 in./yr. This is similar to the subsidence rates seen by level-and-rod and InSAR surveys. The GPS also shows steady state subsidence consistent with InSAR data. It will continue to be an important component of monitoring BM-003. Any deviation from the linear subsidence rate would first be noticed by the wellhead GPS. There have been two large gaps in the GPS data, one in 2016 and another in late 2022 and early 2023. Both instances were because of hardware issues and delays getting new replacement parts.

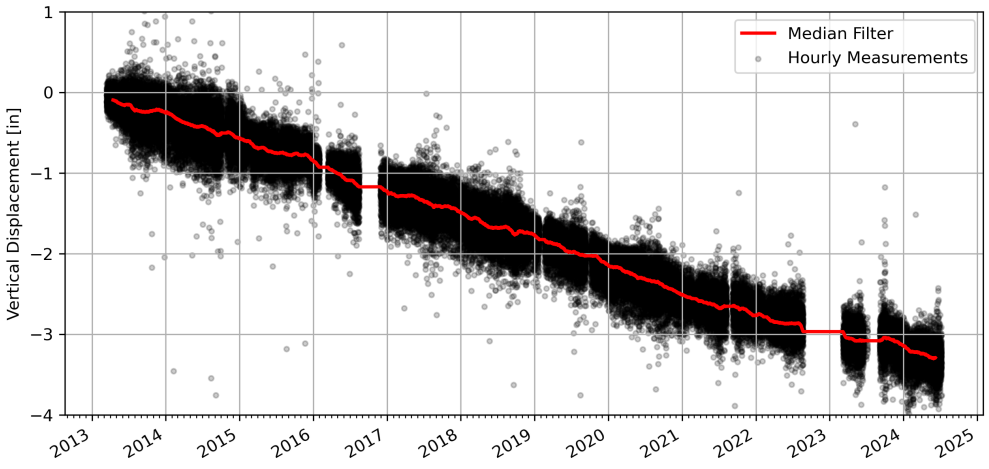

Figure 4-4. Bryan Mound GPS measurements with the gray dots showing hourly measurements and the red line showing a median filter applied to that data.

4.2.2.2. Tiltmeter

In addition to the wellhead GPS, there is also a tiltmeter on the BM-003 wellhead. Data from the tiltmeter are shown in Figure 4-5. There are two measurements shown, tilt to the northern direction in orange and tilt to the eastern direction in blue. Positive northing measurements show tilt to the north while negative northing measurements show southern tilt. Similarly, positive easting measurements show tilt in the easterly direction and negative measurements show tilt to the westerly direction. Both Northing and Easting tilt measurements have two components: 1) the raw data shown as circles, and 2) the filtered data represented with a line. The filtered data uses a median filter with a moving window of one month and is used to remove noise from the system.

Between 2013 and 2021, there was little overall movement at the tiltmeter. In 2021, the tiltmeter began experiencing some movement; however, this movement is still relatively small. According to staff familiar with the tiltmeter, there is no obvious reason the instrument would have been disturbed during that time. It is possible the tiltmeter is beginning to experience seasonal movements. Seasonal movements like these have been seen at other sites like Bayou Choctaw. In addition, there is no obvious correlation to the GPS or InSAR movements.

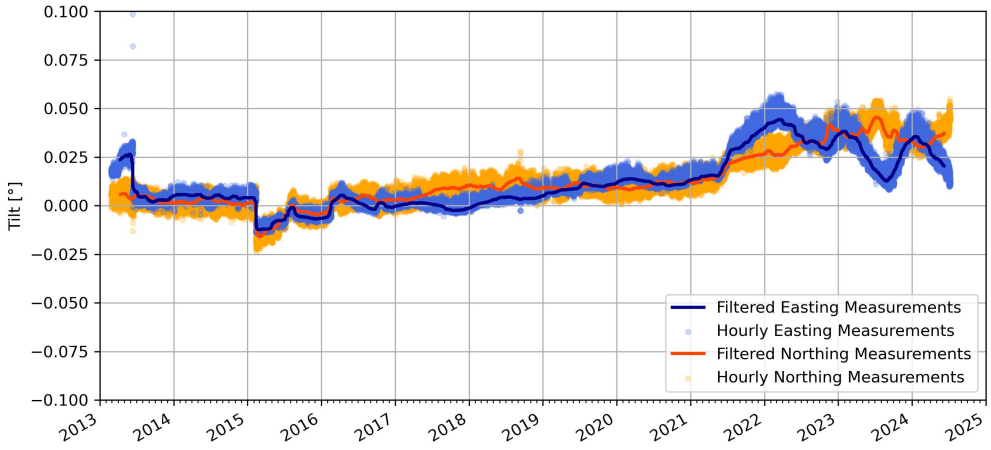

Figure 4-5. Bryan Mound tiltmeter measurements. Northing measurements are shown in orange and easting measurements in blue. Median filters are shown as a line.

4.3. Comprehensive Monitoring

The most crucial area of the site - above BM-003 - is experiencing the highest subsidence at Bryan Mound. Both InSAR and GPS show similar subsidence rates - InSAR shows 0.32 in./yr. over the area while the GPS is estimating 0.30 in./yr. Additionally, both InSAR and GPS are showing linear rates for the area above BM-002 and BM-003. The only contradictory information comes from the wellhead tiltmeter. Since June 2021, the tiltmeter has deviated slightly from its historical pattern.

4.3.1. BM 116A Failure

On May 5, 2024 Bryan Mound well 116A rapidly lost pressure. A high-resolution ultrasonic imaging tool was run soon after. It was found that there was a casing failure at a depth of 983' [13]. A 3D visualization of the dataset at that depth is shown in Figure 4-6. Based on the information in the well survey, it looks as if the casing experienced an axial compression failure. We wanted to see if there were impacts seen at the surface above BM-116 as well as BM-003 because of it's shape and proximity to the well failure. Figure 4-7 shows the proximity between BM-003 and BM-116 [14].

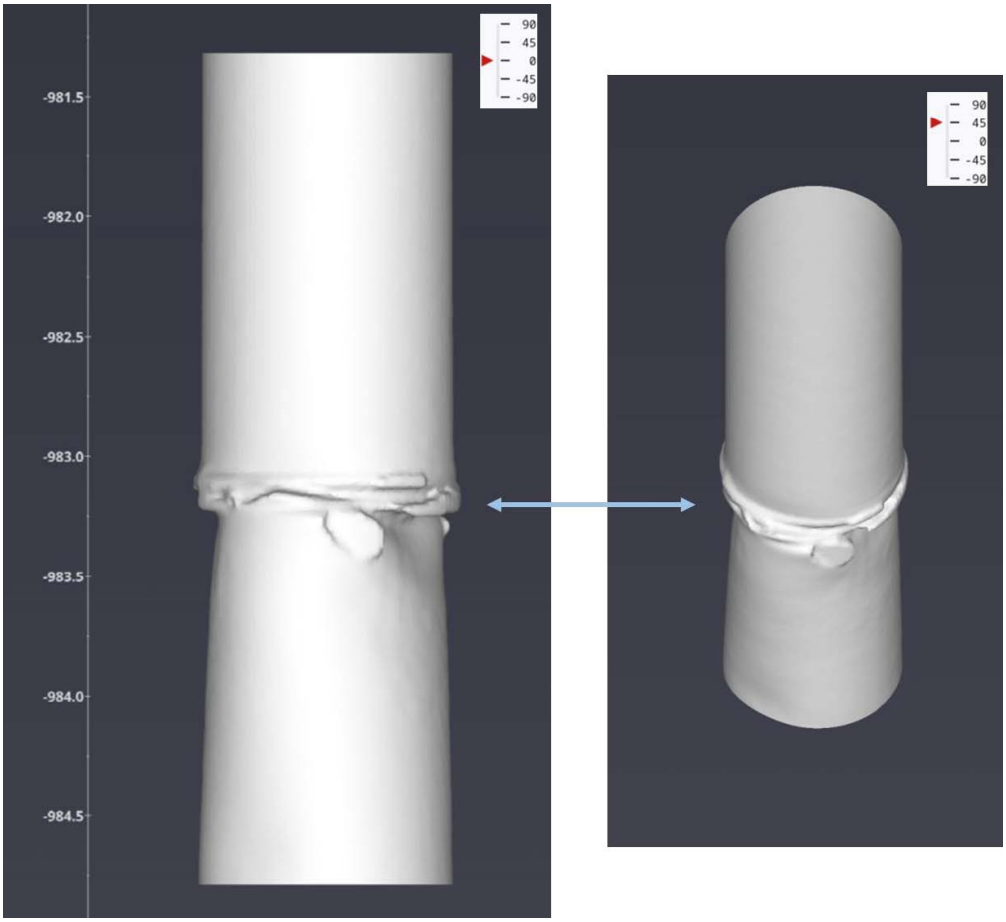

Figure 4-6. 3D visualization of BM-116A using ultrasonic-imaging data at the casing failure. From Mauer 2024.

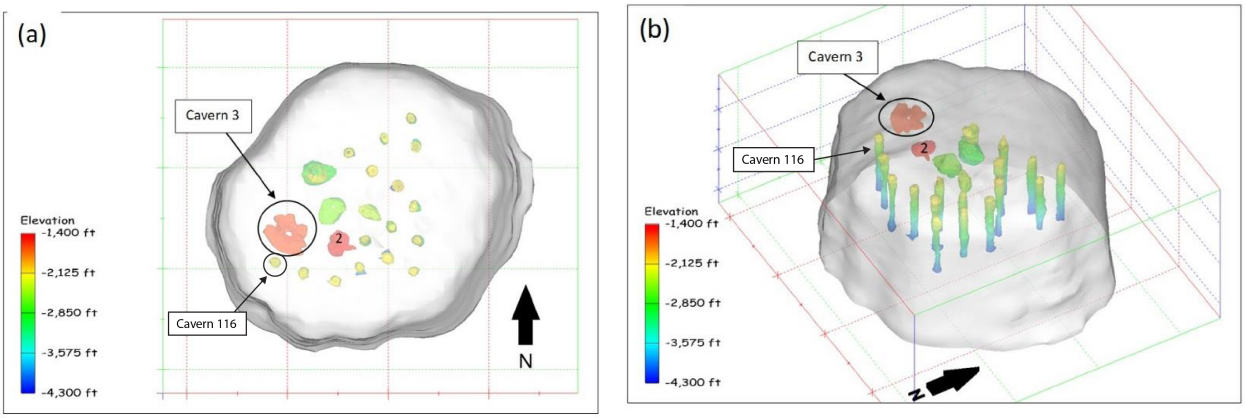

(a) Plan view **(b) View from the southeast.**

Figure 4-7. Bryan Mound salt dome and caverns with Caverns 3 (BM-003) and 116 (BM-116) labeled. Modified from Chojnicki et al., 2017

4.3.1.1. Subsidence Comparison Above BM-003 and BM-116

Figures 4-8 and 4-9 show the comparison between site-wide ground deformation through time at Bryan Mound and individual reflections above BM-116. The filled area shows the extents of surface deformation across the Bryan Mound site. Each variation in color shows the limits of tenth percentile. Darker orange colors represent values closer to the median value. The gray lines show the individual reflections above BM-116. In addition to the measurements there is a dashed red line showing May 5th, the day that BM-116A began losing pressure. Figure 4-8 shows the entire InSAR dataset date range. Most of the reflections above BM-116 hover around the median site values. Figure 4-9 shows just 2024 data. This figure shows slight uplift in some of the individual reflections but follows the site-wide trend.

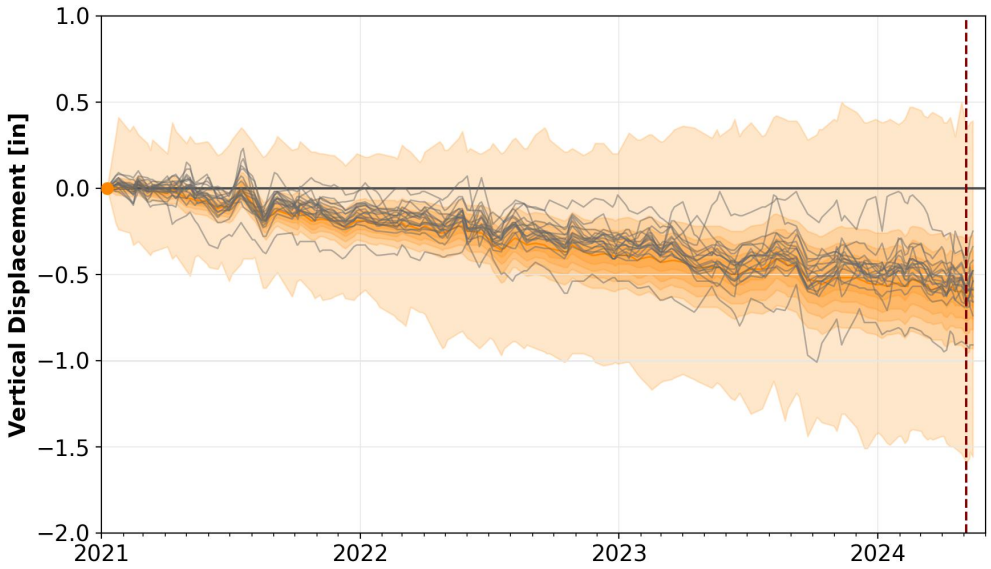

Figure 4-8. Comparison between individual InSAR reflections above BM-116 and site-wide Bryan Mound InSAR results. The gray lines show the individual reflections above BM-116, while the filled area shows the extents of surface deformation across the Bryan Mound site. Each variation in color shows the limits of tenth percentile. Darker orange colors represent values closer to the median value.

Figures 4-10 and 4-11 are similar to the previous figures but show data above BM-003. Surface deformations above BM-003 have always been some of the highest at the site and that is clear when comparing to the site-wide values presented in orange. Similar to the results above BM-116, there is slight uplift seen above the cavern after May 5th, 2024.

Based on the information above BM-116 and BM-003, we do not see anything to suggest that mechanism that caused the BM-116A well failure is being reflected at the surface. It is possible any movement in the subsurface may not be seen for some time. It is also possible that, if the subsurface movement is small, deformation will never be seen at the surface.

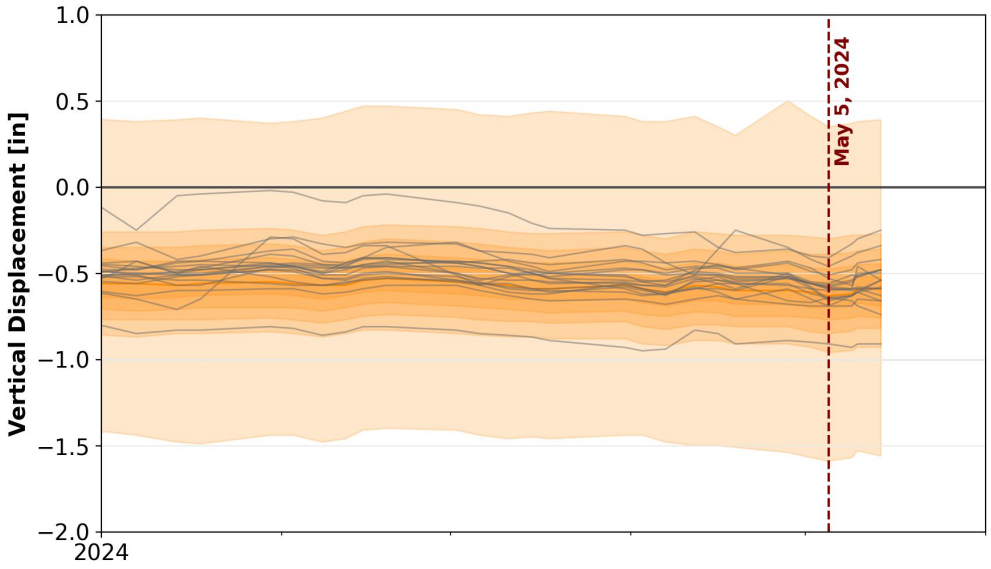

Figure 4-9. Comparison between individual 2024 InSAR reflections above BM-116 and site-wide Bryan Mound InSAR results. The gray lines show the individual reflections above BM-116, while the filled area shows the extents of surface deformation across the Bryan Mound site. Each variation in color shows the limits of tenth percentile. Darker orange colors represent values closer to the median value. Additionally, May 5, 2024 is marked on the figure to show when the well collapse occurred.

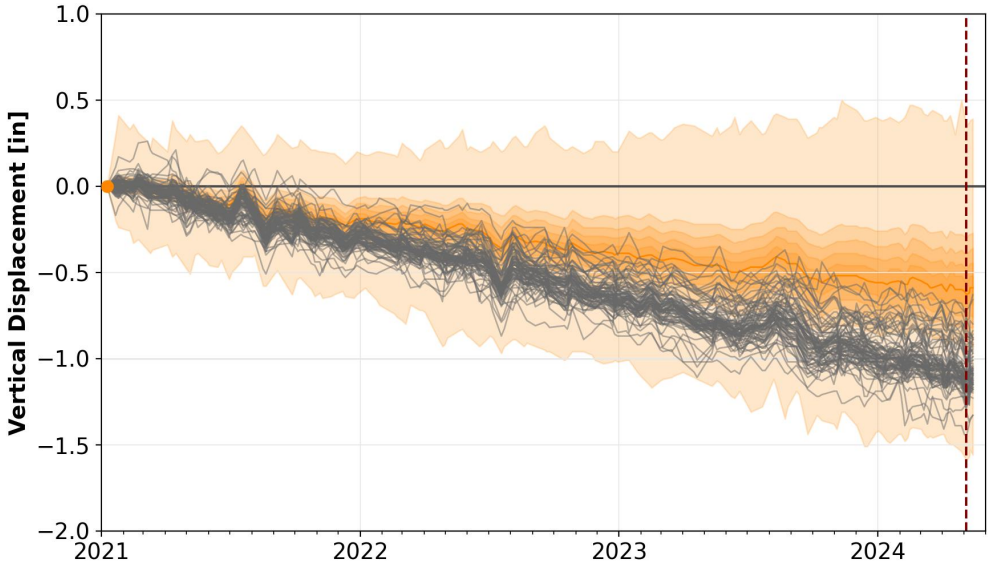

Figure 4-10. Comparison between individual InSAR reflections above BM-003 and site-wide Bryan Mound InSAR results. The gray lines show the individual reflections above BM-003, while the filled area shows the extents of surface deformation across the Bryan Mound site. Each variation in color shows the limits of tenth percentile. Darker orange colors represent values closer to the median value.

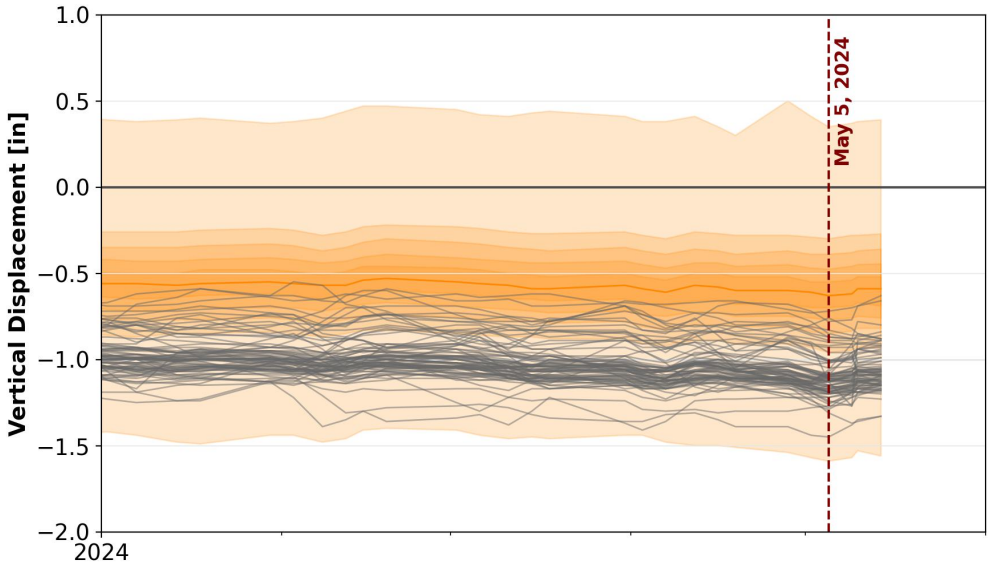

Figure 4-11. Comparison between individual 2024 InSAR reflections above BM-003 and site-wide Bryan Mound InSAR results. The gray lines show the individual reflections above BM-003, while the filled area shows the extents of surface deformation across the Bryan Mound site. Each variation in color shows the limits of tenth percentile. Darker orange colors represent values closer to the median value. Additionally, May 5, 2024 is marked on the figure to show when the well collapse occurred.

4.4. Bryan Mound Conclusions

Bryan Mound has some of the most consistent subsidence of any of the four SPR sites - and this year is no different. The GPS and InSAR data show that subsidence is extremely linear. The tiltmeter only deviates slightly in 2021 but those movements are not seen in the previously mentioned technologies. On May 5th, 2024, BM-116A experienced a likely axial compression failure which caused a rapid depressurization. The mechanism that caused this failure is not currently reflected at the surface but we will continue to monitor the area above 116. Based on the most current surface deformation data, there is no reason to believe that any of the caverns have been structurally compromised.

5. WEST HACKBERRY

5.1. Introduction

West Hackberry has the largest salt dome of the four SPR sites and became operational in 1988. It is located several miles west of Hackberry, LA and shares the dome with two other operators: LA storage and Targa. The SPR site is flanked by LA storage to the west and Targa to the southeast. The subsidence monitoring program at West Hackberry began in 1983 with annual level-and-rod surveys. Since surveying began, West Hackberry has been one of the highest subsiding SPR sites. Although rates are high, there has been no indication that any of the caverns are structurally compromised. One of the more pressing concerns caused by subsidence is the increased flooding potential from the nearby water bodies. During the Life Extension 1 Project, much of the site was changed to increase resilience to flooding. In 2013, operators added a GPS and tiltmeter to supplement the level-and-rod data but both instruments have since been removed. Recently, the SPR has transitioned away from level-and-rod in favor of the satellite-based InSAR.

5.2. Surface Deformation

5.2.1. InSAR

TRE Altamira was contracted to collect, analyze, and report the data. TRE Altamira has experience analyzing SPR sites. They started analyzing Big Hill and Bryan Mound in 2017 and later added Bayou Choctaw and West Hackberry.

InSAR surveys over West Hackberry utilize the TerraSAR-X and PAZ satellites. The TerraSAR and PAZ are sister satellites and have the same acquisition parameters so data from both can be analyzed together. Both satellites are acquiring 1D data in a descending orbit[1]. 1D InSAR measurements survey any deformation directly toward or away from the satellite. This is in contrast to 2D which surveys the site from two different orbits and, subsequently, two different angles. 2D has the ability to measure true vertical movement and East-West movement.

The TerraSAR and PAZ satellites have some of the smallest pixel sizes with a pixel resolution of 3 ft. x 3 ft. The smaller pixel size and higher point density led to tens of thousands of points being surveyed. TRE defines two categories of points: point scatter and distributed scatter. Point scatter is the measurement off a solid reflector within each 3 ft. x 3 ft. pixel. This is generally considered to be more accurate than distributed scatter. Distributed scatter is essentially an average of weaker reflections. For a survey point to be reported it must consistently reflect points throughout the entirety of the survey period. This means that each survey will show the same number of points over the analyzed period.

[1]A descending orbit means the satellite is heading from north to south as it passes over West Hackberry

The area of interest analyzed by TRE Altamira can be seen in Figure 5-1. It covers most of the West Hackberry dome which includes all SPR property. Most of the subsidence is seen on the West Hackberry SPR site. The reference point for the survey is seen off the dome in the southeast corner of the map. This was the most stable point off the dome as determined by TRE Altamira. A closer image of the West Hackberry InSAR data (Figure 5-2) also shows that most of the subsidence is occurring near the center of the cavern field. Specifically, Caverns 101, 103, and 105 have the highest subsidence rates at the site.

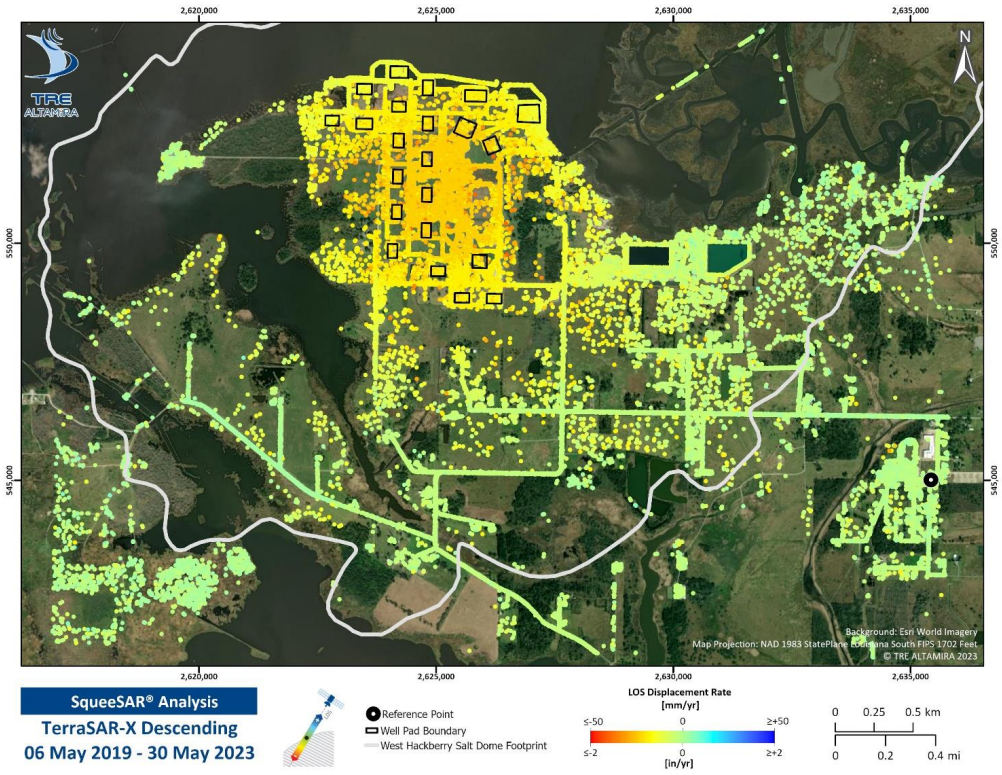

Figure 5-1. 1D InSAR results over the West Hackberry salt dome. Each dot represents a single measured area. Greens are near zero, while the warmer colors show greater subsidence. The reference point for the survey is denoted as a black circle located in the southeast area of the AOI. Well pads at the WH SPR site are shown as black rectangles. From TRE Altamira Report

Average surface deformation rates for all wellpads are presented in Table 5-1. Spatial coverage at the site was similar to last year's survey. The calculated rates are about a tenth of an inch less than the historical level-and-rod surveys. Additionally, the pattern of subsidence seen from InSAR is consistent with historical results – the highest subsidence rates are typically seen near the center of the cavern field. From a geomechanical perspective this is to be expected - as deformation from creep propagates to the surface, it spreads out over an area. In a cavern field these areas of deformation tend to overlap. The middle of the cavern field has the greatest number of overlapping areas of deformation and, therefore, the greatest subsidence.

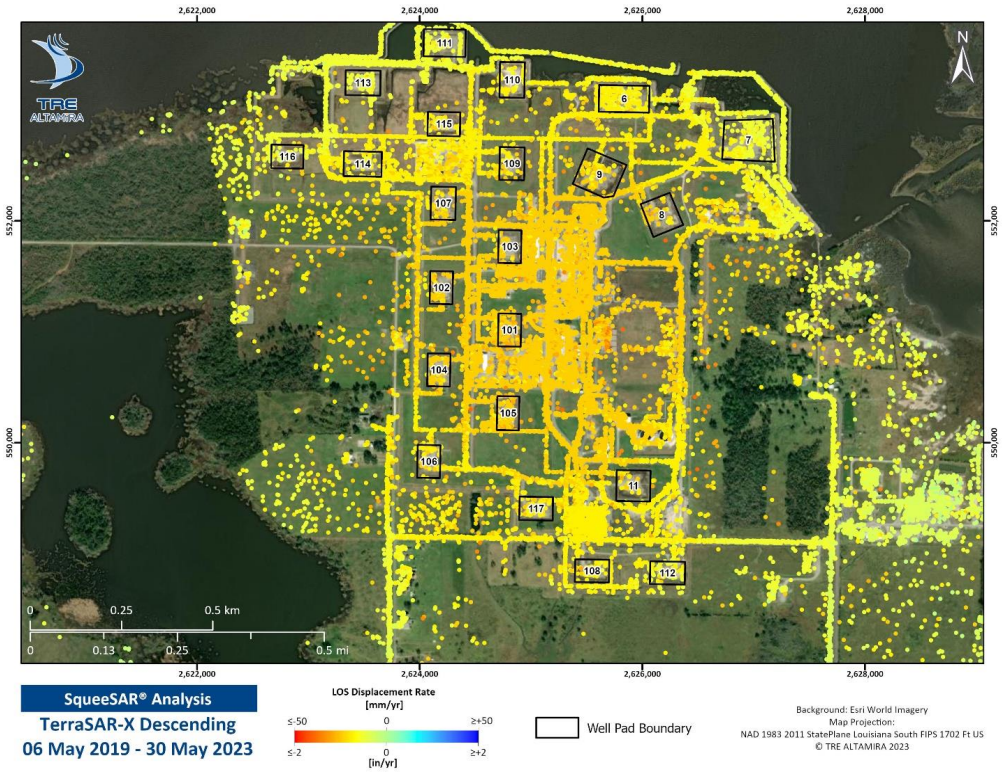

Figure 5-2. 1D InSAR results over the West Hackberry SPR site (2019 – 2022). From TRE Altamira Report

Table 5-1. Average wellpad surface deformation calculated by InSAR

Cavern	Disp. Rate (in./yr.)	Cavern	Disp. Rate (in./yr.)
006	-0.66	107	-0.80
007	-0.56	108	-0.69
008	-0.82	109	-0.79
009	-0.81	110	-0.64
011	-0.78	111	-0.51
101	-0.92	112	-0.61
102	-0.84	113	-0.54
103	-0.87	114	-0.67
104	-0.82	115	-0.71
105	-0.88	116	-0.54
106	-0.74	117	-0.76

5.3. Comprehensive Monitoring

The most notable characteristic about this year's data is the change in subsidence rates that occurred in 2022. Information gathered from InSAR shows that West Hackberry had been subsiding at a relatively linear rate since InSAR collection began. This changed in 2022 when subsidence seems to have increased

at the beginning of the year and then decreased later that year. Historically, West Hackberry has had higher but largely consistent subsidence rates. A change in site subsidence indicates something in the subsurface has changed. The change is not enough to indicate damage to the caverns but we may be able to have a better understanding of the subsurface if we can understand what is driving the changes in subsidence.

5.3.1. Comparing Oil Transfers to Subsidence Rates

Two sites, West Hackberry and Big Hill, both showed changes in subsidence around the same time — which is also around the time of the oil sales. As such, the first approach is to determine if changes in site operations may have contributed to the change in subsidence. At a high level, we want to see whether or not surface velocities change with a change in site operations. This is easier said than done. Although InSAR is accurate and numerous, we are measuring data from a real-world system that can be noisy. We cannot *directly* derive any meaningful velocity from the InSAR data because any noise in the position data will be exacerbated in the corresponding velocity data. Instead, we will need to smooth the InSAR data to approximate surface velocities across the site.

We can smooth the InSAR data using a localized regression method called LOWESS. LOWESS, or **Lo**cally **We**ighted **S**catterplot **S**moothing, is a non-parametric smoothing function that relies on least squares fitting on local regions within the dataset (i.e. it performs a linear estimation on each section of the data to determine the best fit). The best way to characterize the site with a single dataset is with the median subsidence data already presented in Figure 1-1. This dataset was used to perform the LOWESS smoothing. A window of 1/8 of the dataset (approximately six months) was used for the regression. Results from the smoothing algorithm are shown in Figure 5-3. The smoothed data are laid on top of the original displacement data.

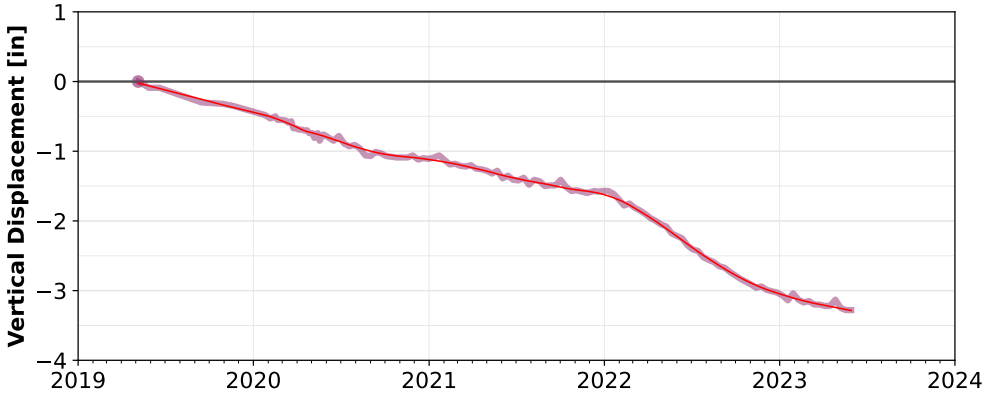

Figure 5-3. Median surface deformation across the West Hackberry SPR site shown in purple with LOWESS smoothing estimation overlaid in red.

Velocity data were subsequently calculated using the smoothed data. The gradient of the smoothed displacement data was calculated using a central difference method. Resulting velocity data are shown in Figure 5-4. The exact point in time where subsidence increased is evident in the velocity data: November 2021. This data can now be compared to site operations.

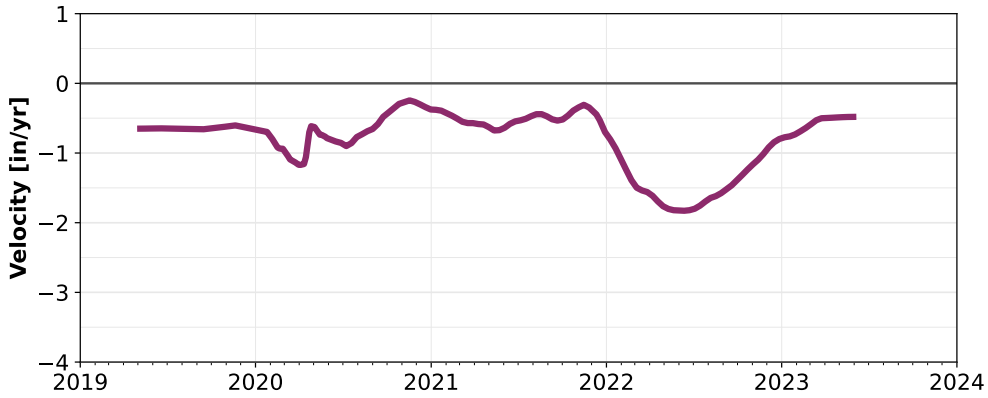

Figure 5-4. Median West Hackberry surface velocity derived from LOWESS smoothing.

While there are many site operations to compare (e.g. oil/brine transfers into or out of caverns, cavern pressures, etc.) site oil transfers out of the caverns by month will serve as a proxy to estimate site operations as a whole. The visual comparison between the monthly oil transfers and the velocity profile is shown in Figure 5-5. The two curves share the same x-axis (time) but the y-axes measure different quantities. The y-axis to the left of the figure in black corresponds to the monthly oil transfers out of the West Hackberry caverns. The y-axis to the right of the figure shows the surface velocity calculated in Figure 5-4 but this time inverted and scaled.

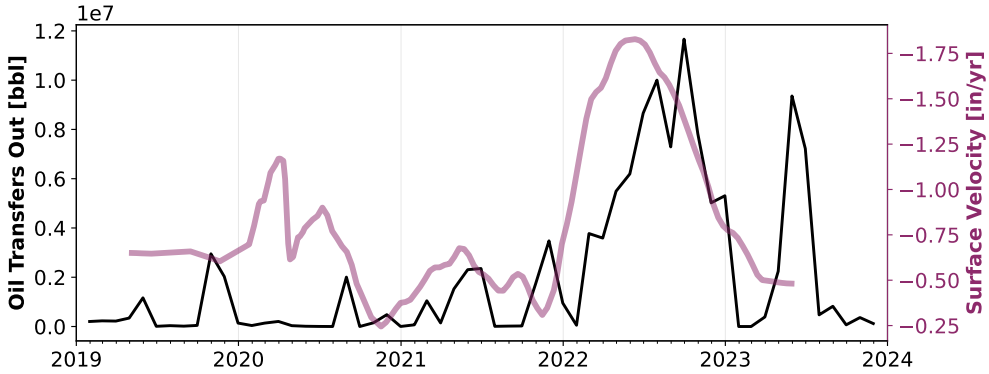

Figure 5-5. Qualitative comparison between oil transfers out (black) and median West Hackberry surface velocity (purple).

Qualitatively, the two curves share a similar shape at corresponding points in time. This may suggest that there is a correlation between oil transfers and increased subsidence at the site; however, there are several other factors that must be considered. These are the same factors discussed in a similar analysis for Big Hill (Section 3.5.1).

5.3.2. Comparing with Cavern Pressure

A more direct comparison may be comparing subsidence rates with cavern pressures; however, this could prove difficult. Each cavern has a different operating pressure and so the analysis would have to be at the

cavern level. At the cavern level, there is the possibility that nearby caverns could impact the subsidence rates in the area above other caverns. This is further complicated by the fact that West Hackberry is a cavern field and there can be multiple overlapping subsidence zones. This effect makes it difficult to isolate the effect of depressuring a single cavern. However, the SPR program has retained these records and this may be the subject of future research.

5.4. West Hackberry Conclusions

Historically, West Hackberry has had the highest subsidence rates of the four SPR sites with the highest rates nearing one inch per year. In 2022, both Big Hill and West Hackberry have experienced greater subsidence rates nearing two inches per year. The most recent InSAR results indicate that subsidence rates have slowed back to pre-2022 levels. It is possible the increased subsidence rates in 2022 are correlated with increased site activity from oil sales; however, there is no evidence to suggest that increased site activity has damaged any of West Hackberry's infrastructure or caverns.

This page intentionally left blank.

BIBLIOGRAPHY

[1] Dylan Moriarty. Strategic petroleum reserve enhanced monitoring compendium - fy 2022, 2022.

[2] Dylan Moriarty. Strategic petroleum reserve enhanced monitoring compendium - fy23, 2023.

[3] Andres Acevedo. Analysis of ground displacements over the bayou choctaw salt dome (september 2023), 2023.

[4] Victor Faraco. Analysis of ground displacements over the bayou choctaw salt dome (december 2023), 2024.

[5] Raquel Valdez and Dylan Moriarty. Assessment of insar seasonal movements at bayou choctaw spr site, 2022.

[6] J. T. Neal, T. R. Magorian, R. L. Thoms, W. J. Auten, R. P. McCulloh, S Denzler, and K. O. Byrne. Anomalous zones in gulf coast salt domes with special reference to big hill, tx, and weeks island, la, 1993.

[7] T. R. Magorian and J. T. Neal. Strategic petroleum reserve (spr) additional geological site characterization studies big hill salt dome, 1988.

[8] C. A. Rautman, K. M. Looff, J. S. Stein, and A. S. Snider. An updated three-dimensional geologic-genetic model of the big hill salt dome and strategic petroleum reserve sit. In *Solution Mining Research Institute, Spring 2005 Technical Conference*, 2005.

[9] D. H. Kupfer. Anomalous feature in the five islands slat stocks. trans., 1990.

[10] B. L. Roberts. Revisions to the strategic petroleum reserve well grading system, 2021.

[11] Victor Faraco. Analysis of ground displacements over the big hill salt dome (april 2024), 2024.

[12] Victor Ciceri. Analysis of ground displacements over the bryan mound salt dome (july 2024), 2024.

[13] Hannah Maurer. Bryan mound collar compression study, 2024.

[14] Kirsten Chojnicki, Anna Lord, and Giorgia Bettin. Cavern abandonment monitoring options letter report, 2017.

This page intentionally left blank.

APPENDIX A.

A.1. Bayou Choctaw Changes in Subsidence Rates

This year's report uses a different reference location than the previous reports. The previous reference monument became unstable and negatively impacted the results. This section is meant to illustrate the difference between data using the previous unstable reference monument and the current monument located in Addis, Louisiana. The ascending datasets were used since they have the largest time coverage and will show the greatest difference of the before and after.

A comparison of the before and after ascending datasets are presented in Figure A-1. The gray and blue areas show the ascending InSAR results with the old and new reference monument, respectively. The areas for the gray and blue areas show the difference between the 5th and 95th percentiles of elevation change through time for their respective datasets. Similarly, the bold lines in those areas show the median values.

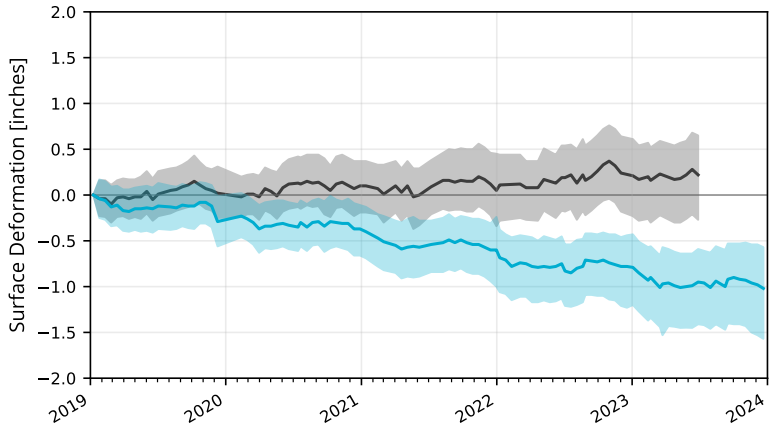

Figure A-1. Comparison between ascending datasets before (gray) and after (blue) reference monument change. The areas represent the extents of the 5th and 95th percentiles while the bold line in the middle shows the median value for elevation change at any given time.

Data collected using the previous reference location (gray area in Figure A-1) indicated elevation gain at the site - there is no physical reason for this to happen. TRE Altamira ultimately determined that the reference location had become unstable. As they were conducting their search for a new reference monument, they realized that most of the old area of interest (AOI) was experiencing similar movement. As such, TRE

Altamira chose to expand the AOI and search for a more stable location farther from the site. They found a suitable location in NE of the site.

The new results show that the Bayou Choctaw site is slowly subsiding. The seasonal pattern still exists but the overall subsidence trend is consistent year-over-year. This is closer to what we would expect from an area near the Gulf Coast. This is a good example of how the reference location plays an important role in the calculation of subsidence rates at any given site. Fortunately, InSAR has the flexibility to change reference points if necessary.

A.2. Bayou Choctaw Tiltmeter Corrections

Sometimes it is necessary to remove a tiltmeter for wellhead maintenance. Each time the tilmeter is reset there is a discontinuity between the measurements pre and post reset. The resulting jump is caused by slight variations in the way the tiltmeter was reinstalled - it is practically impossible to reinstall a tiltmeter with the exact same tilt (or lean) as before. Because of this, the data typically have to be corrected in order to observe any meaningful trends. Corrections listed in the tables below are additions or subtractions to an initial date and all subsequent dates.

Figures A-2 and A-3 show the uncorrected tiltmeter measurements while Tables A-1 and A-2 show the applied corrections to each tiltmeter.

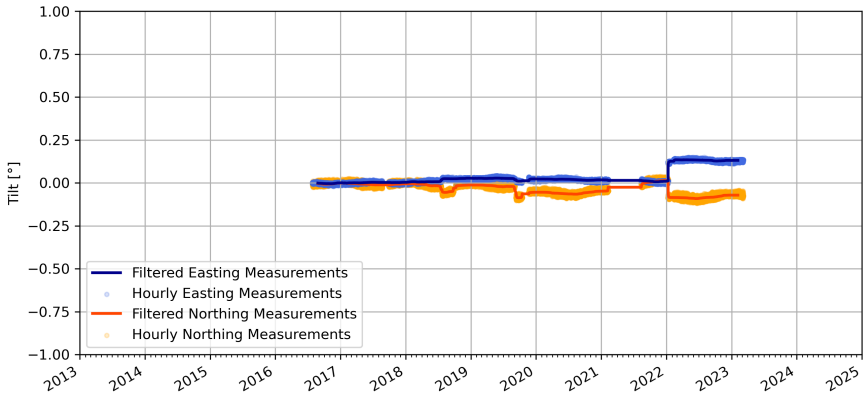

Figure A-2. Uncorrected hourly tiltmeter measurements above Bayou Choctaw Cavern 004. The original northery measurements are shown in orange while the original easting measurements are shown in blue.

Table A-3 shows known outages from the real-time sensing instruments. Each of the instruments are in protective housings but small disturbances can still be seen in the measurements due to the sensitivity of each instrument. For example, large birds roost on the Cavern 004 GPS housing in the winter which leads to temporary negative measurements. Some of the tiltmeter corrections correspond to known outages and resets but the causes for the other jumps are unknown.

Table A-1. Bayou Choctaw Cavern 004 tiltmeter corrections

Begin Date	Easting Adjustment (deg)	Northing Adjustment (deg)
02/09/2016	+0.000	-0.040
07/23/2018	-0.020	+0.037
10/08/2018	+0.000	-0.033
09/11/2019	+0.012	+0.067
11/21/2019	-0.020	-0.025
04/01/2021	+0.010	-0.060
12/30/2021	-0.125	+0.100

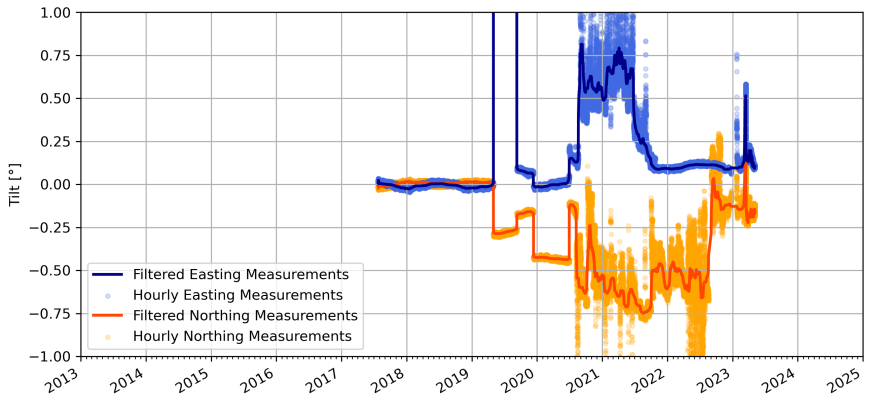

Figure A-3. Uncorrected hourly tiltmeter measurements above Bayou Choctaw Cavern 020. The original northing measurements are shown in orange while the original easting measurements are shown in blue.

Table A-2. Bayou Choctaw Cavern 020 tiltmeter corrections

Begin Date	Easting Adjustment (deg)	Northing Adjustment (deg)
05/01/2019	-2.100	+0.300
09/11/2019	+2.025	-0.090
12/11/2019	+0.080	+0.268
06/29/2020	-0.160	+0.000

Table A-3. Real-time sensing instrument outages

August 22, 2017 to **September 27, 2017 (36 days)** *All instruments* Failure of the control room receiving radio
July 17, 2018 to **July 23, 2018 (6 days)** *BC4 GPS, BC4 Tiltmeter* Removal of Cavern 4 wellhead instruments for sonar
July 25, 2018 to **September 4, 2018 (41 days)** *BC4 GPS, BC20 GPS* Failure of GPS power supply
September 25, 2018 to **October 8, 2018 (13 days)** *BC4 Tiltmeter* Removal of instrument for wireline
September 9, 2019 to **October 28, 2019 (49 days)** *BC20 GPS* Taken offline for routine well maintenance, discovered antenna and powercord were fused together from corrosion, both cables were damaged, and replacements had to be ordered

DISTRIBUTION

Email—Internal

Name	Org.	Sandia Email Address
Technical Library	1911	sanddocs@sandia.gov

Hardcopy—Internal

Number of Copies	Name	Org.	Mailstop
1	Dylan Moriarty	8912	0750

This page intentionally left blank.

Sandia National Laboratories

Sandia National Laboratories is a multimission laboratory managed and operated by National Technology & Engineering Solutions of Sandia LLC, a wholly owned subsidiary of Honeywell International Inc., for the U.S. Department of Energy's National Nuclear Security Administration under contract DE-NA0003525.